

## A point-by-point response to the reviews

Anonymous Referee #1

Received and published: 8 March 2017

The authors presented comprehensive aerosol dataset observed from metropolitan city of Shanghai. The measurements and data are valuable to study nowadays severe haze in China. The authors conclude that the accumulation of local emissions under stagnant meteorological conditions as well as rapid particle growth by secondary processes are primarily responsible for the haze formation in Shanghai. The analysis of particles hygroscopicity and density variations during pollution events is very interesting although no specific mechanism, which is actually very complex in urban areas, is addressed in the study. And also, the authors may need to improve the language. In general, I think the paper is suitable for publication in this special issue after addressing some minor issues as follows,

**Answer:** We sincerely thanks you for your pertinent comments and valuable suggestions. The language has been polished in the revised manuscript.

L36 remove “in heavily polluted areas” .

**Answer:** Revised.

L88 no mechanisms are actually discussed in this paper.

**Answer:** The banana-shaped particle size distribution provide a unique chance to reveal evolutions of particle hygroscopicity and effective density due to particle growth.

Section 2.1, Besides the sampling sites information, the authors also present measurements and data information here.

**Answer:** Revised. Measurements and data information in this section are categorized in another section.

L172 the authors think that the differences among the concentrations of PM<sub>1</sub>, PM<sub>2.5</sub> and PM<sub>10</sub> were insignificant. Is that true? According to the Fig. 2, on 26 Dec, they showed large differences in PM<sub>1</sub>, PM<sub>2.5</sub> and PM<sub>10</sub>.

**Answer:** The statement has been revised as “Generally, the difference between the concentrations of

PM<sub>1.0</sub> and PM<sub>2.5</sub> during clean periods was less significant than that in haze days”.

L176 -177, you mentioned that the PM mass dropped sharply due to the atmospheric dilution or precipitation. Do you have such data to support this?

**Answer:** This conclusion is supported by meteorological data in the revised Figure S1. Detailed description has been added: During the end of each PM episode, the change in weather conditions played a key role in the decrease of particle concentration. As shown in Figure S1, the prevailing winds on haze days were from the northwest. The prevailing winds during two clean periods (December 25-27 and January 12-14) were northeasterly, which bring clean air mass from East China Sea. Two cold fronts from the north swept Shanghai on December 31 and January 6, bringing gale and lower temperature, which favored the dispersion of atmospheric pollutants.

L182, is it 0.28, or 0?

**Answer:** it is 0.28

L202, it seems particles with  $D_p > 300$  nm are with lower kappa, why? Some explanations are needed here.

**Answer:** For 300-400 nm particles, the average Kappa are similar (0.335 for 300 nm, 0.331 for 350 nm, and 0.335 for 400 nm), whereas the 5th percentile  $\kappa$  decreased with increasing size. Additional statement is given as “It is noticeable that the 5th percentile hygroscopicity decreased for dry diameter larger than 300 nm, likely due to the presence of the smallest dust particles (Gasparini et al., 2006)”.

L217: The interpretation “. . .strong formation of sulfate and nitrate” looks contrary with the section 3.2, the section 3.2 shown that SNA (sulfate, nitrate, ammonium) only accounts for 28% of PM<sub>1.0</sub>.

**Answer:** The formation of sulfate and nitrate is stronger compared to the USA site reported by Gasparini et al. (2006). The statement has been revised as “We attribute the different size dependencies of hygroscopicity among various measurement sites to the total emissions of SO<sub>2</sub> and NO<sub>x</sub>, which were responsible for the formation of hygroscopic sulfate and nitrate”.

L235-238: The reviewer is confused that why the number fraction of the lower density group increased as the concentration of NO increase. Did the authors analyze the relationship of them? or any reference?

**Answer:** This feature was reported in two papers. The statement has been revised as: The lower density particles with  $\rho_{\text{eff}} < 1.0 \text{ g cm}^{-3}$  were attributable to fresh or partially aged traffic-related particles, because the number fraction of the lower density group in urban area was found to be consistent with the concentration of NO (indicator of traffic) (Levy et al., 2013; Rissler et al., 2014).

Section 3.3, you talk about Kappa in the first part of this section, but you used GF in the second part. It'd better to use one parameter.

**Answer:** The term “GF” in the second part is replaced by “Kappa” in the revised manuscript.

Fig.3 the authors may look the mass fraction of SIA, but not the mass concentrations. It is of course that the mass of each component will increase with the increase of PM.

**Answer:** The mass fraction of SIA is clearly reflected by linear regressions.

Fig.5 and L259-261, it seems it's difficult to see the characteristics you described here. You may replot the figure to make it more clearly to reviewers.

**Answer:** The particle number concentrations (black line in Figure 5) during haze period varied in the same range as in transition period, indicating little difference. The volume concentration (purple line) in haze days was always higher than that during transition period.

L342-344, is the first banana shape a NPF event? Because you said the other two are not.

**Answer:** The possibility of NPF can be ignored in this observation due to the absence of the burst of nucleation mode particles. Difference between NPF and the three particle growth events has been discussed in detail in the revised manuscript.

L360-371: The science of the analyzing method is weak. Anytime the number fraction and GF of the more-hygroscopic group always increase with particle size (Figure 6).

It's hard to say that the hygroscopicity difference in size was caused by the particle growth. The density difference has also the similar problem.

**Answer:** Indeed, this feature that the GF of the more-hygroscopic group increase with particle size cannot be attributed to particle growth in most cases, because the particles in different size are very likely from

different source. In this observation, particle growth process was clearly displayed by the banana-shaped evolutions of particle size distribution, which provided a unique chance for us to study hygroscopicity evolution due to particle growth.

Section 3.6, it's very interesting to look at the particles hygroscopicity and density evolutions during the particle growth. The authors have investigated the particles with different Dp (40 nm, 100 nm and 220 nm). But to my understand, it may be more reasonable to look the GF and density with same Dp during different stage. For example, how do the GF and density of 100 nm particles changed from initial stage to growth stage?

**Answer:** Temporal variation of GF for a certain size was extensively discussed in previous studies. Different from most studies, one highlight of this work is the particle growth process reflected by the “banana” shape particle size distribution. The objective is to reflect the changes in hygroscopicity and effective density as particle is growing. This statement has been added: The latter two banana-shaped evolutions lasted long enough to tracer the changes in hygroscopicity and effective density due to particle growth.

And also, according to Fig. 7, it seems, during the period 2 and period 3, the concentrations for both the Nitrate and sulfate didn't increase and remain flat trends. How can you say that the secondary sulfate and nitrate was major contributors to particle growth during haze events?

**Answer:** The relative contribution of nitrate determined by the SPAMS (0.2–2.0  $\mu\text{m}$ ) increased visibly as the PM episode developed. Different from the total concentration in SPAMS, the HTDMA test showed that the hygroscopicity increased as the particle grew from 40 nm to 100 nm, revealing hygroscopic SNA contributed greatly to the particle growth from 40 nm to 100 nm particles.

## Reference

Gasparini, R., Li, R. J., Collins, D. R., Ferrare, R. A., and Brackett, V. G.: Application of aerosol hygroscopicity measured at the Atmospheric Radiation Measurement Program's Southern Great Plains site to examine composition and evolution, *J. Geophys. Res.-Atmos.*, 111, D05S12, doi:10.1029/2004JD005448, 10.1029/2004jd005448, 2006.

Levy, M. E., Zhang, R. Y., Khalizov, A. F., Zheng, J., Collins, D. R., Glen, C. R., Wang, Y., Yu, X. Y., Luke, W., Jayne, J. T., and Olaguer, E.: Measurements of submicron aerosols in Houston, Texas during the 2009 SHARP field campaign, *J. Geophys. Res.-Atmos.*, 118, 10518-10534, 10.1002/jgrd.50785, 2013.

Rissler, J., Nordin, E. Z., Eriksson, A. C., Nilsson, P. T., Frosch, M., Sporre, M. K., Wierzbicka, A.,

Svenningsson, B., Londahl, J., Messing, M. E., Sjogren, S., Hemmingsen, J. G., Loft, S., Pagels, J. H., and Swietlicki, E.: Effective density and mixing state of aerosol particles in a near-traffic urban environment, *Environ Sci Technol*, 48, 6300-6308, 10.1021/es5000353, 2014.

Gasparini, R., Li, R. J., Collins, D. R., Ferrare, R. A., and Brackett, V. G.: Application of aerosol hygroscopicity measured at the Atmospheric Radiation Measurement Program's Southern Great Plains site to examine composition and evolution, *J. Geophys. Res.-Atmos.*, 111, D05S12, doi:10.1029/2004JD005448, 10.1029/2004jd005448, 2006.

Gasparini, R., Li, R. J., Collins, D. R., Ferrare, R. A., and Brackett, V. G.: Application of aerosol hygroscopicity measured at the Atmospheric Radiation Measurement Program's Southern Great Plains site to examine composition and evolution, *J. Geophys. Res.-Atmos.*, 111, D05S12, doi:10.1029/2004JD005448, 10.1029/2004jd005448, 2006.

Gasparini, R., Li, R. J., Collins, D. R., Ferrare, R. A., and Brackett, V. G.: Application of aerosol hygroscopicity measured at the Atmospheric Radiation Measurement Program's Southern Great Plains site to examine composition and evolution, *J. Geophys. Res.-Atmos.*, 111, D05S12, doi:10.1029/2004JD005448, 10.1029/2004jd005448, 2006.

Anonymous Referee #2

Received and published: 28 February 2017

In this study, aerosol measurements were performed over about three weeks during winter to understand the causes of severe haze pollution in Shanghai. The measured aerosol properties include particle size distributions, hygroscopicity, effective density, and chemical composition. From the analysis of aerosols, trace gases, and meteorological data, it is concluded that the particle pollution events are caused by the accumulation of local emissions under stagnant meteorological conditions and exacerbated by rapid particle growth via secondary processes. Overall, the study is well executed, data analysis is mostly appropriate, and the paper is reasonably well written. I believe that it would be beneficial to extend the analysis to include several other effects, as detailed below. Also, a number of minor issues need to be addressed before the paper can be accepted for publication.

A recent publication by Wang, G., et al. (Persistent sulfate formation from London Fog to Chinese haze. *Proc. Natl. Acad. Sci. USA* 2016, 113 (48), 13630-13635) has shown that in two other major Chinese cities the aqueous oxidation of SO<sub>2</sub> by NO<sub>2</sub> in the absence of light can lead to efficient sulfate formation on fine aerosols. The process requires high relative humidity and the presence of NH<sub>3</sub>. It is suggested that in heavily polluted environments, this heterogeneous process can form large amounts of particulate sulfate and nitrate in aqueous particles. Do you have photoactinic light intensity measurements to evaluate the relative contributions from photochemical and dark reactions leading to the particle growth? Were

ammonia measurements available for the study period? Can you use particle hygroscopicity measurements reported in your study to derive aerosol state (aqueous/dry) and relate with the particle growth rates? Doing so would bring this study to an entirely new level.

**Answer:** We sincerely thanks you for your pertinent comments and valuable suggestions. The publication by Wang et al (2016) provided a new insight into night formation mechanisms of PM<sub>2.5</sub> and pointed out us the research direction in the future. However, the correlation between particle growth rate and aerosol water content cannot be obtained in this study, because RH-dependent hygroscopic growth was not measured in the observation.

The authors should at least attempt to explain the 5-day cycle. Was it related to the workweek/weekend cycle or something else?

**Answer:** The periodic PM episodes are really unrelated to weekend cycles. Detailed description has been added: During the end of each PM episode, the change in weather conditions played a key role in the decrease of particle concentration. As shown in Figure S1, the prevailing winds on haze days were from the northwest. The prevailing winds during two clean periods (December 25-27 and January 12-14) were northeasterly, which bring clean air mass from East China Sea. Two cold fronts from the north swept Shanghai on December 31 and January 6, bringing gale and lower temperature, which favored the dispersion of atmospheric pollutants.

Minor comments:

L11: Particulate matter (PM) and haze are not synonymous, strictly speaking. The former term is typically used to describe aqueous aerosol particles (deliquesced, but not cloud droplets). These two terms cannot be interchanged; such use creates confusion. I suggest revising the use of haze and PM in the abstract and throughout entire manuscript.

**Answer:** I agree with you that particulate matter and haze are not the same. Particulate matter (PM) are microscopic solid or liquid matter suspended in the atmosphere (<https://en.wikipedia.org/wiki/Particulates>). Generally, haze pollution in china is defined as visibility decrease caused by the increase of fine particulate matter. To avoid confusion, the term “haze episode” was replaced by “haze event” in the revised manuscript.

L15: This sentence may become clearer if re-written as follows: “The mass ratio of SNA/PM1.0 (sulfate, nitrate, and ammonium) fluctuated only slightly around 0.28, suggesting that both secondary inorganic compounds and carbonaceous aerosols contributed substantially to the haze formation, regardless of pollution level.” Also, the original sentence implies that all of the non-SNA material is carbonaceous. Perhaps this must be stated explicitly.

**Answer:** This sentence has been revised following your suggestions.

L77: This statement implies that all traffic particles are soot aggregates, which is not correct

**Answer:** The nascent larger traffic particles are aggregates of primary particles with varying content of semi-volatile material. To avoid confusion, the sentence has been revised as “The effective density of nascent traffic particles varies from approximately  $0.9 \text{ g cm}^{-3}$  to below  $0.4 \text{ g cm}^{-3}$ , decreasing with the increase of particle size, because there are more voids between primary particles in relatively larger aggregates (Momenimovahed and Olfert, 2015).”

L78: Do the authors refer to material density or effective density?

**Answer:** Effective density. Revised.

L85: Must be ‘cascade impactor’ here and throughout the rest of the manuscript

**Answer:** All of them has been revised following your suggestions.

L87: Mass spectrometry is used to measure the particle composition, which is used to infer the particle hygroscopicity and density.

**Answer:** We have not determined the particle hygroscopicity and density by method of chemical closure in this study. Information on particle composition measured in this study can provide some explanation to the variations of particle hygroscopicity and density. The statement has been revised as “cascade impactor samples were collected and temporal variations of particle composition were determined by a single particle mass spectrometry, which provided further insight into the hygroscopicity and density variations.”

L112: HTDMA does not measure the particle number size distribution

**Answer:** Our HTDMA has the function of SMPS. Detail information on this HTDMA can see Ye et al., A multifunctional HTDMA system with a robust temperature control, *Advances in Atmospheric Sciences*, 26 (2009)1235-1240.

L132: ‘. . .Mass SpectrometER’

**Answer:** The official name is Single Particle Aerosol Mass Spectrometry.

L166: these values must be rounded off, e.g.,  $57 \pm 37$

**Answer:** Thanks for your suggestions, the sentence has been revised as “The average concentrations of  $\text{PM}_{1.0}$ ,  $\text{PM}_{2.5}$ , and  $\text{PM}_{10}$  were  $57 \pm 37$ ,  $87 \pm 67$ , and  $129 \pm 78 \mu\text{g m}^{-3}$ , respectively.”

L175: what does 'late' refer to?

**Answer:** The statement has been revised as "During the end of each episode".

L188: This sentence is confusing because it compares the contribution from a chemical (NO<sub>x</sub>) with that from a source of a chemical (presumably SO<sub>2</sub>) – coal-fired power plants. Also, doesn't coal combustion release NO<sub>x</sub> as well? The authors must provide data showing that traffic contributes more to the NO<sub>x</sub> burden than the power plants and other industrial sources that utilize coal.

**Answer:** Indeed, coal combustion release NO<sub>x</sub>, although NO<sub>x</sub> emission decreased significantly due to the full implement of flue gas deNO<sub>x</sub> in power plants. To avoid confusion, the statement has been revised as "This indicated that NO<sub>x</sub> contributed more to haze formation in Shanghai compared to SO<sub>2</sub>."

L194: what does 'their' refer to?

**Answer:** The statement has been revised as "due to different atmospheric lifetimes among SO<sub>2</sub>, NO<sub>x</sub>, and VOCs".

L195: Isn't sulfate also of secondary origin?

**Answer:** Sulfate is certainly of secondary origin. However, regional transport is a big source of SO<sub>2</sub>. So, sulfate is excluded from secondary transformation of local emissions.

L209: The meaning of this sentence is unclear. Why was hygroscopicity limited to smaller sizes? Do you mean 'measurements were limited to sizes smaller than 250 nm'?

**Answer:** The statements has been revised as "Generally, HTDMAs measure dry particles smaller than 300 nm due to technical limitations, and it is common that particle hygroscopicity increases with increase of particle size (Liu et al., 2014;Swietlicki et al., 2008)."

L226: replace 'contradictory' with 'opposite'

**Answer:** Revised.

L240: Insert a reference to Figure 2 early on in this paragraph

**Answer:** Revised as "As shown in Figure 2".

L282: Not all VOCs react with ozone. Can you provide data on the concentration of unsaturated organics?

**Answer:** The concentration of unsaturated organics is not available in this studies.

L286: ‘. . .were less- and some that were more’ - what?

**Answer:** The statement has been revised as ”the nearly-hydrophobic particles were externally mixed with some hygroscopic particles”.

L304 and several other instances: ‘less-massive’ – did you mean ‘lower density’?

**Answer:** the term ‘lower density’ is replaced by ‘less-massive’ in the revised manuscript.

L381: ‘. . .contributed substantially. . .because the . . .ratio was almost constant. . .’ – this is an invalid argument. The second part does not follow from the first part.

**Answer:** The statement has been revised as “Both secondary inorganic salts and carbonaceous aerosols contributed substantially to haze formation, because the mass ratio of SNA/PM<sub>1.0</sub> fluctuated slightly around 0.28 during the observation period.”

Figure 2: explain in figure caption the meaning of the dashed line

**Answer:** Revised.

Figure 3: What is ‘SIA’ in figure legend. Use a secondary Y-axis for the SIA/PM ratio

**Answer:** Revised following your suggestions.

Reference:

Liu, H. J., Zhao, C. S., Nekat, B., Ma, N., Wiedensohler, A., van Pinxteren, D., Spindler, G., Müller, K., and Herrmann, H.: Aerosol hygroscopicity derived from size-segregated chemical composition and its parameterization in the North China Plain, *Atmospheric Chemistry and Physics*, 14, 2525-2539, 10.5194/acp-14-2525-2014, 2014.

Momenimovahed, A., and Olfert, J. S.: Effective density and volatility of particles emitted from gasoline direct injection vehicles and implications for particle mass measurement, *Aerosol Sci. Technol.*, 49, 1051-1062, 10.1080/02786826.2015.1094181, 2015.

Swietlicki, E., Hansson, H. C., Hameri, K., Svenningsson, B., Massling, A., McFiggans, G., McMurry, P. H., Petaja, T., Tunved, P., Gysel, M., Topping, D., Weingartner, E., Baltensperger, U., Rissler, J., Wiedensohler, A., and Kulmala, M.: Hygroscopic properties of submicrometer atmospheric aerosol particles measured with H-TDMA instruments in various environments - a review, *Tellus Ser. B-Chem. Phys. Meteorol.*, 60, 432-469, 10.1111/j.1600-0889.2008.00350.x, 2008.

## The list of all relevant changes made in the manuscript

The line numbers are based on the ACPD version.

Line 9: “haze event from a series of periodic” was deleted

Line 10-12: “Particle size distribution, hygroscopicity, and effective density were measured online, along with analysis of water-soluble inorganic ions and single particle mass spectrometry.” was revised as “Particle size distribution, hygroscopicity, effective density and single particle mass spectrometry were determined online, along with offline analysis of water-soluble inorganic ions”

Line 12-15: “Regardless of pollution level, the mass ratio of SNA/PM<sub>1.0</sub> (sulfate, nitrate, and ammonium) slightly fluctuated around 0.28 over the whole observation, suggesting that both secondary inorganic compounds and carbonaceous aerosols (including soot and organic matter) contributed substantially to the haze formation.” was revised as “The mass ratio of SNA/PM<sub>1.0</sub> (sulfate, nitrate, and ammonium) fluctuated slightly around 0.28, suggesting that both secondary inorganic compounds and carbonaceous aerosols contributed substantially to the haze formation, regardless of pollution level”

Line 16: “During the representative PM episode,” was added.

Line 16-18: “The calculated PM concentration from particle size distribution displayed a variation pattern similar to that of measured PM<sub>1.0</sub> during the representative PM episode,” was revised as “the calculated PM was always consistent with the measured PM<sub>1.0</sub>,”

Line 18: “the” was added between “that” and “enhanced”

Line 20: “the” was added after “indicating”; “banana-shape” was revised as “banana-shaped”

Line 21: “in PM<sub>1.0</sub>” was revised as “of PM<sub>1.0</sub>”; we added “that the” and “the” before “rapid size growth” and “condensation” respectively.

Line 24: “the” was added after “that”

Line 24-25: “NO<sub>x</sub> and SO<sub>2</sub> was a major contributor to the particle growth” was revised as “NO<sub>x</sub> and SO<sub>2</sub> was one of the most important contributors to the particle growth”

Line 32: “as well as strong impacts” was revised as “Also, atmospheric aerosol has strong impacts”

Line 33-34: “in heavily polluted areas” was deleted.

Line 63: “haze episodes” was revised as “haze events”

Line 64: “in contrast that primary emissions” was revised as “in contrast with the fact that primary emissions”

Line 65: “haze episodes” was revised as “haze events”

Line 81: “haze episodes” was revised as “haze events”

Line 82: “in the high level of sulfate during haze episodes” was revised as “about the high level of sulfate during haze events”; “It is revealed by” was revised as “It was revealed by”; “the” was added after “that”

Line 87: “which was” was revised as “as”

Line 96: “the” was added before “temporal”

Line 99: “hygroscopicity have helped the explanation of haze formation mechanisms in Beijing and Shanghai” was revised as “hygroscopicity has thrown some new light on haze formation mechanisms in Beijing and Shanghai”

Line 103-104: “effective densities of traffic particles are below  $1.0 \text{ g cm}^{-3}$ , and density decreases with the increase of particle size because there are more voids between primary particles in relatively larger aggregates” was revised as “effective densities of nascent traffic particles varies from approximately  $0.9 \text{ g cm}^{-3}$  to below  $0.4 \text{ g cm}^{-3}$ , decreasing with the increase of particle size, because there are more voids between primary particles in relatively larger aggregates”

Line 105: “density” was revised as “effective density”

Line 111-112: “cascade samples were collected and a single particle mass spectrometry was used to better understand the hygroscopicity and density variations” was revised as “cascade impactor samples were

collected and temporal variations of particle composition were determined by a single particle mass spectrometry, which provided further insight into the hygroscopicity and density variations”

Line 114: “haze episodes” was revised as “haze events”

Line 118: “The measurements” was revised as “The measurements of particle hygroscopicity and effective density”

Line 119-120: “a representative urban site close to a sub-center of Shanghai” was revised as “It can be considered as a representative urban site for Shanghai”.

Line 120: “There are many dwelling quarters and commercial blocks in surrounding area. About 400 m away from the measurement site, there is the Middle Ring Line, one of the busiest elevated roads in the city.” was added.

Line 120-127: A new section 2.2 “Measurements of air quality index and ground meteorological parameters” was added. “At a supersite about 100 m away” was revised as “At a supersite about 100 m away from the Environmental Building.”; “The concentrations of PM<sub>2.5</sub>, PM<sub>10</sub>, and CO” was revised as “The datas of PM<sub>2.5</sub>, PM<sub>10</sub>, and CO”

Line 128: “2.2. HTDMA-APM system” was revised as “2.3. HTDMA-APM system”

Line 154: “2.3. SPAMS” was revised as “2.4. SPAMS”

Line 165: “2.4. Ion chromatography” was revised as “2.5. Ion chromatography”

Line 166 and line 169: “Cascade aerosol samples” and “cascade samples” were revised as “Cascade impactor aerosol samples” and “cascade impactor samples”

Line 183: “PM<sub>1.0</sub>, PM<sub>2.5</sub>, and PM<sub>10</sub> were 57.3±37.0, 87.2±67.2, and 127.8±77.7 μg m<sup>-3</sup>” was revised as “PM<sub>1.0</sub>, PM<sub>2.5</sub>, and PM<sub>10</sub> were 57±37, 87±67, and 129±78 μg m<sup>-3</sup>”

Line 187-188: “During the clean period, the differences among the concentrations of PM<sub>1.0</sub>, PM<sub>2.5</sub>, and PM<sub>10</sub> were insignificant” was revised as “Generally, the difference between the concentrations of PM<sub>1.0</sub> and PM<sub>2.5</sub> during clean days was less significant than that in haze periods”

Line 189-192: “During the late episodes, the PM mass loading abruptly dropped, due to change in the atmospheric dilution or wet deposition.” was revised as “During the end of each PM episode, the change in weather conditions played a key role in the decrease of particle concentration. As shown in Figure S1, the prevailing winds on haze days were from the northwest. The prevailing winds during two clean periods (December 25-27 and January 12-14) were northeasterly, bringing clean air mass from East China Sea. Two cold fronts from the north swept Shanghai on December 31 and January 6, bringing gale and lower temperature which favored the dispersion of atmospheric pollutants”

Line 200: “episodes” was replaced with “events”

Line 201-202: “This indicated that NO<sub>x</sub> contributed more to haze formation in Shanghai than did coal-fired sources” was revised as “This finding indicates that NO<sub>x</sub> contributed more to haze formation in Shanghai compared to SO<sub>2</sub>.”

Line 204: “haze episodes” was revised as “haze events”

Line 207: “the” was added after “with”

Line 208-209: “This finding suggests that the haze formation mechanism is likely different in Shanghai and Beijing.” was revised as “This finding suggests that the haze formation mechanism in Shanghai is likely different from that in Beijing”

Line 211: “due to their different atmospheric lifetimes” was revised as “due to different atmospheric lifetimes among SO<sub>2</sub>, NO<sub>x</sub>, and VOCs”

Line 215: “median hygroscopicity” was revised as “mean hygroscopicity”

Line 217: “with an average  $\kappa$  of” was revised as “with a mean  $\kappa$  of”; “the”

Line 224: “Generally, the HTDMA-measured hygroscopicity was limited to the size range below 250 nm, and it is common that the GF increases with increase of particle size.” was revised as “Generally, HTDMAs measure dry particles smaller than 300 nm due to technical limitations, and it is common that particle hygroscopicity increases with the increase of particle size (Liu et al., 2014;Swietlicki et al., 2008).”.

Line 225: “aerosol hygroscopicity” was replaced with “particle hygroscopicity”

Line 227: “The very few measurements for dry particles larger than 300 nm showed different size dependencies.” was added into this part; “the GF first increase” was revised as “particle hygroscopicity”

Line 228: “In contrast, Wu et al. (2016c) reported that particle hygroscopicity increased with particle diameter in the range of 35-350 nm.” was added.

Line 229: “no decrease in GF was observed” was revised as “the mean  $\kappa$ s of 300, 350 and 400 nm particles were nearly equal.”

Line 229-230: “We attribute the different hygroscopicity to the large emissions of SO<sub>2</sub> and NO<sub>x</sub> in China, which were responsible for the strong formation of sulfate and nitrate.” was revised as “We attribute the different size dependencies of hygroscopicity among various measurement site to the total emissions of SO<sub>2</sub> and NO<sub>x</sub>, gas precursors of hygroscopic sulfate and nitrate.”

Line 230: “It is noticeable that the 5<sup>th</sup> percentile hygroscopicity decreased for dry diameter larger than 300 nm, likely due to the presence of the smallest dust particles.” was added into this part.

Line 231: “variation” was replaced with “variability”

Line 233: “indicated” was replaced with “indicates”

Line 236: “The size distribution of particle density varied in the literature.” was revised as “The size dependency of particle effective density varied in the literature.”

Line 237: “particle density” was revised as “effective density” and “contradictory” was replaced with “opposite”

Line 238-239: “The difference was attributable to the contribution of fresh traffic particles” was revised as “The different trends were attributable to the variable fraction of lower density mode particles ( $\rho_{\text{eff}} < 1.0 \text{ g cm}^{-3}$ )”

Line 239: “The densities of the secondarily produced (NH<sub>4</sub>)<sub>2</sub>SO<sub>4</sub>, NH<sub>4</sub>HSO<sub>4</sub>, and NH<sub>4</sub>NO<sub>3</sub> are ~1.75 g

cm<sup>-3</sup>. The effective density of organic aerosols varies mostly in the range of 1.2-1.6 g cm<sup>-3</sup>, depending on their source origins (Malloy et al., 2009;Turpin and Lim, 2001;Dinar et al., 2006). The lower density particles with  $\rho_{\text{eff}} < 1.0 \text{ g cm}^{-3}$  were attributable to fresh or partially aged traffic-related particles, because the number fraction of the lower density group in urban area was found to be consistent with the concentration of NO (indicator of traffic) (Levy et al., 2013;Rissler et al., 2014).” was added.

Line 240-241: “emissions from traffic exhaust” was replaced with “traffic emissions”

Line 242-243: “reported that a quasi-monodisperse density distribution was dominant for accumulation mode particles” was revised as “reported that effective density distributions were dominated by a single peak in the previous observation”

Line 243-247: “externally mixed aerosols with a lower density group ( $\rho_{\text{eff}} = \sim 1.0 \text{ g cm}^{-3}$ ) were often present in this observation, and were responsible for the decrease of the mean effective density. The lower effective density group was attributed to fresh or slightly aged traffic-related particles, because the number fraction of the lower density group increased as the concentration of NO increased.” was revised as “a lower density peak below  $1.0 \text{ g cm}^{-3}$  was often present in this observation, decreasing the mean effective density of externally mixed aerosols.”

Line 249: “As shown in Figure 2,” was added.

Line 251: “clean” was replaced with “clean period”

Line 257-258: “Figure 5 displays the temporal evolution of particle size distribution in comparison with the measured PM<sub>1.0</sub> concentration during the representative PM episode” was revised as “Figure 5 displays the temporal profile of particle size distribution, along with the measured PM<sub>1.0</sub> concentration during the representative PM episode”

Line 260: “It is noticeable that the temporal trends in mass concentrations of PM<sub>cal</sub> and PM<sub>1.0</sub> are highly consistent.” was added into this part.

Line 265-266: “The difference of total number concentration between transition and haze periods was insignificant,” was revised as “The difference of particle number concentration between transition and haze periods was less significant,”

Line 266: “rapidly” was replaced with “considerably”

Line 271: “This indicates” was revised as “This finding indicates”

Line 287: “near- hydrophobic” was replaced with “the near-hydrophobic”

Line 302, 304 and 308: “less-massive” was replaced with “lower density”

Line 324: “As shown in Figure 5,” was added; “banana-shape” was revised as “banana-shaped”

Line 335: “The burst of Aitken mode particles was” was revised as “The burst of Aitken mode particles in the current study may be”

Line 337: “banana-shape” was revised as “banana-shaped”

Line 337-338: “were primarily caused by coagulation and condensation growth” was revised as “particle growth in the time evolution of particle size distribution from the Aitken mode size range to accumulation mode size range was primarily due to coagulation and condensation growth.”

Line 338: “growth” was revised as “processes”; “which provided” was revised as “This feature provided”

Line 340,342,346: “banana-shape” was revised as “banana-shaped”

Line 345: “continuous increase” was revised as “a continuous increase”

Line 347: “with continuous increase” was revised as “with the continuous increase”

Line 348: “The latter two banana-shaped evolutions lasted long enough to tracer the changes in hygroscopicity and effective density due to particle growth.” was added.

Line 369: “cascade samples” was revised as “cascade impactor samples”

Line 372: “ $87.2 \pm 67.2 \mu\text{g m}^{-3}$ ” was revised as “ $87 \pm 67 \mu\text{g m}^{-3}$ ”

Line 374: “because the SNA/PM<sub>1.0</sub> ratio was almost constant during the observation period” was revised

as “because the mass ratio of SNA/PM<sub>1.0</sub> fluctuated slightly around 0.28 during the observation period.”

Line 377-378: “which caused a large accumulation” was revised as “which favored the”

Line 382: “was a major contributor to particle growth” was revised as “one of the most important contributors to particle growth”

Line 670: Figure 2 was replaced with a modified one. The caption of PM =75  $\mu\text{g m}^{-3}$  was added into the new figure.

Line 673-676: Figure 3 was replaced with a modified one. A y axis for SNA/PM<sub>1.0</sub> was added into the new figure.

## The marked-up manuscript

# Insight into winter haze formation mechanisms based on aerosol hygroscopicity and effective density measurements

Yuanyuan Xie<sup>1</sup>, Xingnan Ye<sup>1,2\*</sup>, Zhen Ma<sup>1</sup>, Ye Tao<sup>1</sup>, Ruyu Wang<sup>1</sup>, Ci Zhang<sup>1</sup>, Xin Yang<sup>1,2</sup>, Jianmin Chen<sup>1,2\*</sup>, Hong Chen<sup>1</sup>

<sup>1</sup>Shanghai Key Laboratory of Atmospheric Particle Pollution and Prevention (LAP<sup>3</sup>), Department of Environmental Science and Engineering, Fudan University, Shanghai 200433, China.

[<sup>2</sup>Institute of Atmospheric Sciences, Fudan University, Shanghai 200433, China.](#)

\*Correspondence to: Xingnan Ye (yexingnan@fudan.edu.cn), Jianmin Chen (jmchen@fudan.edu.cn).

**Abstract:** We characterize a representative ~~haze event from a series of periodic~~ particulate matter (PM) episodes that occurred in Shanghai during winter 2014. Particle size distribution, hygroscopicity, [effective density](#) and ~~effective density~~ [single particle mass spectrometry](#) were ~~measured~~ [determined](#) online, along with [offline](#) analysis of water-soluble inorganic ions ~~and single particle mass spectrometry~~. ~~Regardless of pollution level,~~ [T](#)he mass ratio of SNA/PM<sub>1.0</sub> (sulfate, nitrate, and ammonium) ~~slightly~~ [slightly](#) fluctuated around 0.28, ~~over the whole observation,~~ suggesting that both secondary inorganic compounds and carbonaceous aerosols (~~including soot and organic matter~~) contributed substantially to the haze formation.

~~regardless of pollution level.~~ Nitrate was the most abundant ionic species during hazy periods, indicating that  $\text{NO}_x$  contributed more to haze formation in Shanghai than did  $\text{SO}_2$ . ~~During the representative PM episode, the calculated PM concentration from particle size distribution displayed a variation pattern similar to that of~~ was always consistent with the measured  $\text{PM}_{1.0}$ . ~~during the representative PM episode,~~ indicating that the enhanced pollution level was attributable to the elevated number of larger particles. The number fraction of the near-hydrophobic group increased as the PM episode developed, indicating the accumulation of local emissions. Three “banana-shaped” particle evolutions were consistent with the rapid increase ~~of in~~  $\text{PM}_{1.0}$  mass loading, indicating that the rapid size growth by the condensation of condensable materials was responsible for the severe haze formation. Both hygroscopicity and effective density of the particles increased considerably with growing particle size during the banana-shaped evolutions, indicating that the secondary transformation of  $\text{NO}_x$  and  $\text{SO}_2$  was one of the most important ~~major~~ contributors to the particle growth. Our results suggest that the accumulation of gas-phase and particulate pollutants under stagnant meteorological conditions and subsequent rapid particle growth by secondary processes, were primarily responsible for the haze pollution in Shanghai during wintertime.

**Keywords:** air pollution; size distribution; hygroscopic growth; secondary process; Shanghai.

## 1. Introduction

Atmospheric aerosol has significant influences on radiation balance and climate forcing of the

atmosphere (Wang et al., 2011;Wang et al., 2014c;Wu et al., 2016a;IPCC, 2013); Also, atmospheric aerosol has as well as strong impacts on visibility (Yang et al., 2012;Lin et al., 2014;Xiao et al., 2014) and public health (Heal et al., 2012) in heavily polluted areas. Recent studies found that short-term exposure to haze pollution could cause airway inflammation and aggravate respiratory symptoms in chronic obstructive pulmonary disease patients (Wu et al., 2016b;Guan et al., 2016).

With the huge achievements in economic development and rapid urbanization over the past 30 years, particulate pollution has become a major environmental concern in China. The most severe haze event that occurred in the first quarter of 2013, spread over 1.6 million km<sup>2</sup> (Wang et al., 2014a). This event motivated the release of the Action Plan on Prevention and Control of Air Pollution with the goal of reducing PM<sub>2.5</sub> (particulate matter smaller than 2.5 μm in aerodynamic diameter) concentration by 15–25% in 2017 against 2012 in three major city clusters ([http://english.mep.gov.cn/News\\_service/infocus/201309/t20130924\\_260707.htm](http://english.mep.gov.cn/News_service/infocus/201309/t20130924_260707.htm)). In order to reduce the PM<sub>2.5</sub> concentration, extensive studies have been conducted to investigate the sources and formation mechanisms of haze pollution in recent years (Ye et al., 2011;Sun et al., 2016;Qiao et al., 2016;Hu et al., 2016;Li et al., 2016;Guo et al., 2014;Zheng et al., 2015;Guo et al., 2013;Wang et al., 2016;Peng et al., 2016). However, the haze formation mechanisms and source appointment of fine particles remain uncertain.

Guo et al. (2013) summarized historical reports from 2000 to 2008 in Beijing and found that the

origins of urban fine particles varied in different seasons: the contribution of primary emissions is comparable to that of secondary formation during winter heating periods whereas secondarily produced aerosols dominate the fine PM sources in other seasons. As an important type of primary emissions in urban area, black carbon (BC) is primarily from incomplete fossil fuel combustion. Light absorption of BC aerosols is increased after atmospheric aging by coating with secondary materials and restructuring (Khalizov et al., 2009). Due to cooling effect at the surface and warming effect aloft, the enhanced light absorption and scattering by aged BC particles stabilize the atmosphere, hindering vertical transport of gaseous and particulate pollutants (Wang et al., 2013). BC aging occurs much more efficiently in the presence of highly elevated gaseous aerosol precursors so that light absorption increases by a factor of 2.4 within 4.6 h under highly polluted conditions in Beijing, significantly exacerbating pollution accumulation and strongly contributing to severe haze formation (Peng et al., 2016).

Due to the implement of several effective regulatory policies, the increasing trend of primary emissions has been under control since the 11<sup>th</sup> five-year period. A growing number of studies suggested that secondary production was the major contributor to the haze [event episodes](#) in recent years (Shi et al., 2014; Zhao et al., 2013; Zhang et al., 2015a; Huang et al., 2014), in contrast [with the fact](#) that primary emissions were of great importance in some haze [event episodes](#) (Niu et al., 2016). Guo et al. (2014) reported that the development of PM episodes in Beijing was characterized by efficient nucleation and continuous particle growth over an extend period dominated by local secondary formation. They

attributed the continuous growth of particle size and constant accumulation of particle mass concentration to the highly elevated concentrations of gaseous precursors such as  $\text{NO}_x$ ,  $\text{SO}_2$ , and volatile organic compounds (VOCs), while the contribution from primary emissions and regional transport was negligible. However, the role of regional transport of  $\text{PM}_{2.5}$  in haze formation remains controversial (Li et al., 2015; Zhang et al., 2015b).

The most important advances in the understanding of urban PM formation were reviewed by Zhang et al. (2015c). The concentrations of  $\text{SO}_2$ ,  $\text{NO}_x$ , and anthropogenic source VOCs in Beijing and other cities of the developing world are significantly higher than those in the urban areas of developed countries, resulting in large secondary production of sulfate, nitrate, and SOA. Synergetic effects among various organic and inorganic compounds may exist under highly polluted conditions, indicating different PM formation rates between developing and developed urban regions. Indeed, a large enhancement of particulate sulfate was typically observed during regional haze events in China (Chen et al., 2016; Wang et al., 2015; Fu et al., 2008; Xie et al., 2015). Currently, the highly elevated sulfate concentration during haze [event episodes](#) cannot be fully explained by model simulations (Wang et al., 2014b; Chen et al., 2016). Recently, a significant breakthrough made by Wang et al. (2016) has provided a reasonable explanation [about](#) the high level of sulfate during haze [event episodes](#). It [was](#) revealed by their laboratory experiments that [the](#) aqueous oxidation of  $\text{SO}_2$  by  $\text{NO}_2$  proceeds more efficiently with the increase of  $\text{NO}_2$  concentration whereas the reaction is suppressed in acid conditions, because acid effect

reduces the solubility of SO<sub>2</sub> and reaction rate. The enhanced sulfate formation during severe haze periods in Beijing was attributable to aqueous oxidation of SO<sub>2</sub> by NO<sub>2</sub> on hygroscopic fine particles under conditions of elevated RH and the concentrations of NH<sub>3</sub> and NO<sub>2</sub>, ~~as which was~~ confirmed by the comparable SO<sub>2</sub> uptake coefficients for sulfate formation from field and laboratory results.

The hygroscopic properties of ambient particles vary significantly depending on the origin of the air masses and the atmospheric aging process. In urban air, the population of near-hydrophobic particles can be assumed to consist largely of freshly emitted combustion particles containing high mass fractions of soot and water-insoluble organic compounds (Swietlicki et al., 2008; Massling et al., 2009). In contrast, secondary sulfate or nitrate aged particles are more-hygroscopic, and their relative abundance is primarily responsible for the hygroscopic growth of ambient particles at elevated RH (Topping et al., 2005; Aggarwal et al., 2007; Gysel et al., 2007). Thus, hygroscopicity can serve as a tracer of source origins, mixing state, and aging mechanisms of ambient particles. For example, ~~the~~ temporal variations of aerosol hygroscopicity ~~has thrown some new light on~~ ~~have helped the explanation of~~ haze formation mechanisms in Beijing and Shanghai (Ye et al., 2011; Guo et al., 2014).

Density is one of the most important physicochemical properties for atmospheric aerosols. Effective density has served as a tracer for new particle formation and for the aging process in previous studies (Yin et al., 2015; Guo et al., 2014). The ambient particles in urban areas are mostly complex mixtures of elemental carbon (EC), organics (OC), and secondary inorganic aerosols (SIA) (Hu et al., 2012). The

effective densities of nascent traffic particles varies from approximately 0.9 g cm<sup>-3</sup> to below 0.4 g cm<sup>-3</sup>, are below 1.0 g cm<sup>-3</sup>, and density decreases decreasing with the increase of particle size, because there are more voids between primary particles in relatively larger aggregates (Momenimovahed and Olfert, 2015). The effective density of OC is in between those of EC and SIA, and varies with source. The effective density of combustion particles increases by filling the voids in the agglomerate particles with condensed semi-volatile materials, or by restructuring agglomerates with hygroscopic SIA (Momenimovahed and Olfert, 2015; Zhang et al., 2008).

In this study, a combined HTDMA-APM system was used to investigate the variations of hygroscopicity and effective density of submicrometer aerosols during winter 2014 in urban Shanghai. In addition, cascade impactor samples were collected and temporal variations of particle composition were determined by a single particle mass spectrometry, which provided further insight into ~~—was used to better understand~~ the hygroscopicity and density variations. The primary objectives of this study were to investigate the particle growth mechanisms and to identify the contribution of local emissions during the winter haze eventepisode.

## 2. Experimental

### 2.1. Sampling site

The measurements of particle hygroscopicity and effective density were conducted from December 21,

2014 to January 13, 2015 at the Department of Environmental Science and Engineering in the main campus of Fudan University (31.30°N, 121.5°E). It can be considered as a representative urban site for close to a sub-center of Shanghai (Ye et al., 2010). There are many dwelling quarters and commercial blocks in surrounding area. About 400 m away from the measurement site, there is the Middle Ring Line, one of the busiest elevated roads in the city.

## 2.2 Measurements of air quality index and ground meteorological parameters

At a supersite about 100 m away from the Environmental Building, PM<sub>1.0</sub> was monitored using a Thermo Scientific™ 5030 SHARP monitor. Trace gas pollutants were monitored using Thermo Scientific™ i-series gas analyzers (43i for SO<sub>2</sub>, 49i for O<sub>3</sub>, 42i for NO/NO<sub>2</sub>/NO<sub>x</sub>), and meteorological data were monitored using an automatic meteorological station (Model CAWS600, Huayun Inc., China) (Yin et al., 2015). The dataseoncentrations of PM<sub>2.5</sub>, PM<sub>10</sub>, and CO were released by the Shanghai Environmental Monitoring Center. The height of the Planet Boundary Layer (PBL) was computed online using the NCEP Global Data Assimilation System (GDAS) model (<http://ready.arl.noaa.gov/READYamet.php>).

### 2.23. HTDMA-APM system

Particle size distribution, hygroscopic growth factor (GF), and effective density were measured using a custom-built HTDMA-APM system (Figure 1). The custom-built HTDMA (Hygroscopic Tandem Differential Mobility Analyzers) mainly consist of two long DMAs (3081L, TSI Inc.), a humidifier (PD-

50T-12MSS, Perma Pure Inc.) and a Condensation Particle Counter (CPC, Model 3771, TSI Inc.). A detailed description of the HTDMA is available in Ye et al. (2009). In this observation, particle number size distribution in the range of 14–600 nm and hygroscopic growth at 83% RH for particles with dry diameters of 40, 100, 220, 300, 350, and 400 nm were determined by HTDMA (in turn). The determination of effective density by DMA-APM was described previously (Yin et al., 2015; Pagels et al., 2009). Briefly, a combined system consisting of a compact Aerosol Particle Mass Analyzer (APM, Model 3601, Kanomax Inc.) and a CPC (Model 3775, TSI Inc.) was connected to the sample tubing through a 3-way electrical switch behind the upstream DMA (DMA1). The APM comprises two coaxial cylindrical electrodes rotating at the same angular velocity. Charged aerosol particles of a certain diameter sized by DMA1 are axially fed into the annular gap between the electrodes and experienced an outward centrifugal force from the particle rotating and an inward electrostatic force from the high-voltage field between the electrodes. Particles pass through the APM and are sent to the CPC when the two forces are balanced. The mass of particles that pass through the APM is determined by the rotation rate and the applied voltage. Effective densities for dry diameters of 40, 100, 220, and 300 nm were determined by the method of DMA-APM in this study. The HTDMA-APM was operated alternatively in HTDMA mode and then DMA-APM mode, for every 40 min.

Before the field observation, the HTDMA-APM was calibrated using 40–450 nm NIST-Traceable PSL particles and ammonium sulfate. The measured HTDMA data were inversed with the  $TDMA_{inv}$  algorithm

to obtain the actual GF distribution. This is because the raw data are only a skewed and smoothed integral transform of the actual growth factor probability density function (GF-PDF) (Gysel et al., 2009). The hygroscopicity parameter  $\kappa$  was derived from the GF data after inversion with the TDMA<sub>inv</sub> algorithm according to the  $\kappa$ -Köhler theory (Petters and Kreidenweis, 2007).

### **2.43. SPAMS**

A Single Particle Aerosol Mass Spectrometry (SPAMS, Hexin Analytical Instrument Co., Ltd., China) installed in the same room with the HTDMA-APM system was used to obtain the chemical and size information of individual particles in the range of 0.2-2  $\mu\text{m}$ . Detailed information on SPAMS is available in Li et al. (2011). Briefly, ambient particles are drawn into a vacuum chamber through an aerodynamic focusing lens and accelerated to a size-dependent terminal velocity. Sized particles are desorbed and ionized by the pulsed desorption/ionization laser (Q-switched Nd: YAG,  $\lambda=266$  nm) at the ion source region. Both positive and negative mass spectra for a single particle are recorded by a bipolar time-of-flight spectrometer. The single particle information was imported into YAADA (version 2.11, [www.yaada.org](http://www.yaada.org)). Based on the similarities of the mass-to-charge ratio and peak intensity, particles were classified using the ART-2a method.

### **2.54. Ion chromatography**

Cascade [impactor](#) aerosol samples for offline analysis were collected at the roof platform of the Environmental Building using a 10-stage MOUDI sampler (Micro-Orifice Uniform Deposit Impactor,

Model 110-NR, MSP Corp., USA). Detailed description of the sampling, pretreatment, chemical analysis, and quality control of this system is available in Tao et al. (2016). Briefly, cascade [impactor](#) samples were collected every 24 h using the PALL7204 quartz filter as the collection substrate. Each filter was weighed with a BP211D electronic balance at  $25\pm 1^\circ\text{C}$  and  $40\pm 2\%\text{RH}$ . The water extract of each sample was analyzed using an Ion Chromatograph (Metrohm 883 basic IC plus, Switzerland) equipped with a third-party column heater (CT-100, Agela Corp., China). Seven anions ( $\text{F}^-$ ,  $\text{Cl}^-$ ,  $\text{NO}_2^-$ ,  $\text{Br}^-$ ,  $\text{NO}_3^-$ ,  $\text{SO}_4^{2-}$  and  $\text{PO}_4^{3-}$ ) were resolved using a Metrosep A Supp 5-250/4.0 column at  $35^\circ\text{C}$  with an eluent of  $3.2\text{ mmol L}^{-1}\text{ Na}_2\text{CO}_3$  +  $1.0\text{ mmol L}^{-1}\text{ NaHCO}_3$ . Six cations ( $\text{Li}^+$ ,  $\text{Na}^+$ ,  $\text{NH}_4^+$ ,  $\text{K}^+$ ,  $\text{Ca}^{2+}$ , and  $\text{Mg}^{2+}$ ) were separated by a Metrosep C4-250/4.0 column at  $30^\circ\text{C}$  with an eluent of  $1.7\text{ mmol L}^{-1}\text{ HNO}_3$  +  $0.7\text{ mmol L}^{-1}$  2,6-pyridine dicarboxylic acid.

### 3. Results and discussion

#### 3.1. Periodic cycle of PM episodes during the observation period

Figure 2 shows the temporal variations of PM mass loading during the winter observation (December 21, 2014 to January 13, 2015). The official data of  $\text{PM}_{2.5}$  and  $\text{PM}_{10}$  were blank on some clean days. Meteorologically, our measurement was deployed in a typical winter period. The average concentrations of  $\text{PM}_{1.0}$ ,  $\text{PM}_{2.5}$ , and  $\text{PM}_{10}$  were  $57.3\pm 37.0$ ,  $87.2\pm 67.2$ , and  $129.1\pm 27.8\pm 7877.7\text{ }\mu\text{g m}^{-3}$ , respectively. About 62% of hourly averaged  $\text{PM}_{2.5}$  concentrations exceeded  $75\text{ }\mu\text{g m}^{-3}$  of the Chinese Grade II guideline (GB

3095-2012), indicating heavy particle pollution in Shanghai during wintertime. The PM episodes exhibited a clear periodic cycle of ~5 days. A similar feature was previously observed in Beijing (Guo et al., 2014). At the beginning of each cycle, the PM<sub>1.0</sub> level was below 35 µg m<sup>-3</sup>. Generally, the difference between the concentrations of PM<sub>1.0</sub> and PM<sub>2.5</sub> during clean days was less significant than that in haze periods. During the clean period, the differences among the concentrations of PM<sub>1.0</sub>, PM<sub>2.5</sub>, and PM<sub>10</sub> were insignificant. Occasionally the measured PM<sub>2.5</sub> concentrations were larger than those of PM<sub>10</sub>, possibly due to system error. However, the particle mass concentration began to increase in the next few days, with PM<sub>1.0</sub> and PM<sub>2.5</sub> peaking at over 100 and 200 µg m<sup>-3</sup>, respectively. During the end of each PM episode, the change in weather conditions played a key role in the decrease of particle concentration. As shown in Figure S1, the prevailing winds on haze days were from the northwest. The prevailing winds during two clean periods (December 25-27 and January 12-14) were northeasterly, bringing clean air mass from East China Sea. Two cold fronts from the north swept Shanghai on December 31 and January 6, bringing gale and lower temperature which favored the dispersion of atmospheric pollutants. late episodes, the PM mass loading abruptly dropped, due to change in the atmospheric dilution or wet deposition.

### **3.2 Contributions of secondary inorganic aerosols to PM<sub>1.0</sub> mass loading**

Figure 3 illustrates the daily concentrations of sulfate, nitrate, and ammonium as a function of PM<sub>1.0</sub> mass loading. In general, the sum of concentrations of sulfate, nitrate, and ammonium (SNA) increased linearly as PM<sub>1.0</sub> mass loading increased. It is noticeable that the SNA/PM<sub>1.0</sub> ratio slightly fluctuated

around 0.28, regardless of the pollution level. Because soil dust and sea salt made a negligible contribution to the fine particle mass concentration in this study, the almost constant ratio of SNA/PM<sub>1.0</sub> indicates that SNA and carbonaceous aerosols (including soot and organic matter) synchronously increased during [the haze event episodes](#). As the PM<sub>1.0</sub> concentration increased, the concentration of nitrate increased more rapidly than sulfate so that it became the most abundant ionic species at PM<sub>1.0</sub> > 40 µg m<sup>-3</sup>. This [finding indicates](#) that NO<sub>x</sub> contributed more to haze formation in Shanghai [compared to SO<sub>2</sub> than did coal-fired sources](#). Generally, the visibility decreased with the increase in PM concentration, indicating photochemical activity began to weaken as the development of haze [event episodes](#). The large increase in nitrate concentration may be attributable to heterogeneous reaction on the preexisting particles. Nitrate formation is highly dependent on the surface area of preexisting particles and is favored under NH<sub>3</sub>-rich conditions (Chu et al., 2016). In contrast, Han et al. (2016) reported that the mass ratio of nitrate to sulfate decreased with [the](#) increase of PM<sub>2.5</sub> level and that the sources of sulfate contributed more to [the](#) haze formation in Beijing than mobile sources. This finding suggests that the haze formation mechanism [in Shanghai](#) is likely different [from that in in Shanghai and Beijing](#). VOCs and NO<sub>x</sub> are exclusively from local emissions whereas regional transport is a big source of [SO<sub>2</sub>](#) under stagnant atmosphere, due to [their](#) different atmospheric lifetimes [among SO<sub>2</sub>, NO<sub>x</sub>, and VOCs](#) (Guo et al., 2014). Considering the relatively smaller contribution of sulfate, our results reveal that the accumulation and secondary transformation of local emissions likely played a dominant role in this haze formation.

### 3.3 Aerosol hygroscopicity and effective density during the observation period

Figure 4a displays a box chart of the meanmedian hygroscopicity of each hygroscopic growth factor distribution for different sizes. Considering all of the growth factor distributions collectively, the hygroscopicity parameter  $\kappa$  increased with increase of the dry diameter, with a meann-average  $\kappa$  of 0.161 at 40 nm and 0.338 at 300 nm. Assuming a two-component system of a model salt (ammonium sulfate,  $\kappa_m = 0.53$ ) and an insoluble species ( $\kappa = 0$ ), the volume fraction of hygroscopic species ( $\varepsilon$ ) can be obtained based on the Zdanovsldi-Stokes-Robinson (ZSR) mixing rule. The average  $\varepsilon$  was 0.3 for 40 nm particles, suggesting that the primary particles or initial growth of freshly generated particles were dominated by non-hygroscopic species. In contrast, the 300 nm particles were extremely aged, with more-hygroscopic species.

Generally, ~~the HTDMAs measured~~ dry particles smaller than 300 nm due to technical limitations hygroscopicity was limited to the size range below 250 nm, and it is common that particle hygroscopicity increases with the ~~the GF increases with~~ increase of particle size (Liu et al., 2014; Swietlicki et al., 2008). The increase of particleaerosol hygroscopicity with size was attributed to the addition of more-hygroscopic SNA (Swietlicki et al., 2008; Ye et al., 2010). The very few measurements for dry particles larger than 300 nm showed different size dependencies. Gasparini et al. (2006) reported that particle hygroscopicity ~~the GF~~ first increased and then decreased with increase of particle size, peaking at the diameter of 300 nm. In contrast, Wu et al. (2016c) reported that particle

hygroscopicity increased with particle diameter in the range of 35-350 nm. In this study, the determination size range was extended to 400 nm and the mean  $\kappa$ s of 300, 350 and 400 nm particles were nearly equal. ~~decrease in GF was observed.~~ We attribute the different size dependencies of hygroscopicity among various measurement sites to the total emissions of SO<sub>2</sub> and NO<sub>x</sub>, gas precursors of hygroscopic sulfate and nitrate. large emissions of SO<sub>2</sub> and NO<sub>x</sub> in China, which were responsible for the strong formation of sulfate and nitrate. It is noticeable that the 5<sup>th</sup> percentile hygroscopicity decreased for dry diameter larger than 300 nm, likely due to the presence of the smallest dust particles. The variability ~~variation~~ of hygroscopicity parameter  $\kappa$  was much greater for 40 nm particles. The particle population with  $\kappa < 0.1$  was attributed to fresh traffic particles (Ye et al., 2013). The considerable percentile of  $\kappa < 0.1$  indicates ~~se~~ that the 40 nm particle population was sometimes dominated by near-hydrophobic particles.

Figure 4b displays a box chart of median effective density for different particle sizes. The median effective density varied in the narrow range of  $\rho_{\text{eff}} = 1.35\text{--}1.41 \text{ g cm}^{-3}$  for 40–300 nm particle population. The size dependency ~~distribution~~ of particle effective density varied in the literature. Hu et al. (2012) and Yin et al. (2015) reported that effectiveparticle density increased as particle size increased while a opposite~~contradictory~~ trend was observed by Geller et al. (2006) and Spencer et al. (2007). The different trends were~~difference was~~ attributable to the variable fraction of lower density mode particles ( $\rho_{\text{eff}} < 1.0 \text{ g cm}^{-3}$ )~~contribution of fresh traffic particles.~~ The densities of the secondarily produced (NH<sub>4</sub>)<sub>2</sub>SO<sub>4</sub>, NH<sub>4</sub>HSO<sub>4</sub>, and NH<sub>4</sub>NO<sub>3</sub> are  $\sim 1.75 \text{ g cm}^{-3}$ . The effective density of organic aerosols varies mostly in the

range of 1.2-1.6 g cm<sup>-3</sup>, depending on their source origins (Malloy et al., 2009; Turpin and Lim, 2001; Dinar et al., 2006). The lower density particles with  $\rho_{\text{eff}} < 1.0 \text{ g cm}^{-3}$  were attributable to fresh or partially aged traffic-related particles, because the number fraction of the lower density group in urban area was found to be consistent with the concentration of NO (indicator of traffic) (Levy et al., 2013; Rissler et al., 2014). Although the dominant accumulation mode particles have an effective density greater than Aitken mode ones, the presence of a lower effective density group associated with ~~emissions from~~ traffic ~~emissions-exhaust~~ might decrease the mean effective density to a value lower than that of Aitken mode particles (Levy et al., 2014). Yin et al. (2015) reported that effective density distributions were dominated by a single peak in the previous observation~~a quasi-monodisperse density distribution was dominant for accumulation mode particles~~. In contrast, a lower density peak below  $1.0 \text{ g cm}^{-3}$  was often present in this observation, decreasing the mean effective density of externally mixed aerosols~~externally mixed aerosols with a lower density group ( $\rho_{\text{eff}} \approx 1.0 \text{ g cm}^{-3}$ ) were often present in this observation, and were responsible for the decrease of the mean effective density~~. The lower effective density group was attributed to fresh or slightly aged traffic related particles, because the number fraction of the lower density group increased as the concentration of NO increased.

### **3.4 Characteristics of a representative PM episode**

As shown in Figure 2, ~~T~~the PM episode from January 7 to 12 was a representative case of severe haze formation and elimination processes. It can be divided into clean (January 7), transition (January 8), haze

(January 9–11), and post-haze (January 12) periods. During the transition from the clean to haze period (January 7 to 8), both  $PM_{1.0}$  and  $PM_{2.5}$  concentrations increased slightly, with an average  $PM_{1.0}/PM_{2.5}$  ratio of 0.65. A sharp increase in  $PM_{2.5}$  (of  $125 \mu\text{g m}^{-3}$ ) was observed from 6:00 to 12:00 local time on the morning of January 9. During the haze period, the concentration of  $PM_{2.5}$  exceeded  $115 \mu\text{g m}^{-3}$  (medially polluted level, HJ633-2012) for 63 h. On January 11, the hourly  $PM_{2.5}$  concentration exceeded  $250 \mu\text{g m}^{-3}$ , corresponding to the severely polluted level.

Figure 5 displays the temporal ~~profile evolution~~ of particle size distribution, ~~along with~~ ~~in~~ ~~comparison with~~ the measured  $PM_{1.0}$  concentration during the representative PM episode. The calculated PM concentrations ( $PM_{\text{cal}}$ ) were obtained based on the particle size distribution and average effective density of  $1.39 \text{ g m}^{-3}$  in the range of 14–600 nm measured in this study. It is noticeable that the temporal trends in mass concentrations of  $PM_{\text{cal}}$  and  $PM_{1.0}$  are highly consistent. In contrast to the fact that particle size distribution was dominated by nanoparticles during the clean period, the burst of Aitken mode particles and subsequent continuous growth to approximately 200 nm in diameter was observed three times during the haze period, indicating that the presence of numerous larger particles is likely responsible for the severe particle pollution (Guo et al., 2014). The importance of larger particles in haze formation is also illustrated by the contour plot of the particle volume size distribution. The difference of particle ~~total~~ number concentration between transition and haze periods was less significant, ~~insignificant~~, whereas the volume concentration increased considerably ~~rapidly~~ during the haze period. This feature clearly

demonstrates that the haze formation was closely correlated with particle growth and elevated number of larger particles.

Interestingly, the particle mass concentration was sensitive to variations of wind speed and planetary boundary layer (PBL). During the transition and haze periods, the wind speed decreased considerably with insignificant change in prevailing wind (Figure S1). This [finding](#) indicates that outside transportation became less and less significant. It is noteworthy that the temporal evolution of the particle mass concentration was inversely correlated with the PBL height. The decreasing PBL provided a stagnant atmosphere that favored the accumulation of local emissions. This finding reveals that the severe haze pollution was likely triggered by the adverse meteorological conditions. The impact of decreasing PBL height on haze formation can also be evidenced by the variations of trace gaseous species (Figure S2). During the PM episode, the concentrations of NO<sub>2</sub>, SO<sub>2</sub>, and CO displayed variation trends similar to that of the particle concentration. The fluctuations of trace gas concentrations were caused by primary emission and secondary processes. Noticeably, the concentration of NO increased dramatically in rush hours during the haze period, whereas it fluctuated slightly during the clean period; indicating that local emissions were easily accumulated under stagnant atmosphere. In addition, the maximum concentration of O<sub>3</sub> remained considerably higher during daytime, whereas it decreased significantly at night. The most plausible explanation is that O<sub>3</sub> was consumed rapidly by the accumulating trace gases, such as NO<sub>x</sub>, and VOCs.

### 3.5 Variations of hygroscopicity and effective density during the PM episode

Figure 6 shows the averaged hygroscopicity and effective density for different pollution periods of the PM episode. Regardless of the pollution period, [the](#) near-hydrophobic particles were externally mixed with some hygroscopic particles. During the clean period, the more-hygroscopic particles dominated the 40 nm particle population, indicating that the near-hydrophobic primary particles were rapidly dispersed due to atmospheric dilution. The number fraction of the near-hydrophobic group for different sizes increased as the PM episode developed, indicative of the increasing accumulation of local emissions. Notably, the increase of the near-hydrophobic particles with the evolution of the PM episode become less significant as particle size increased, indicating that primary emission exerted a more significant impact on smaller particles than on larger ones. The median diameter of nascent traffic particles from various gasoline sources ranged between 55 and 73 nm with an average of 65 nm (Momenimovahed and Olfert, 2015). Therefore, the number fraction of the near-hydrophobic particles larger than 200 nm is not sensitive to the accumulation of traffic emissions.

Interestingly, the variations of particle effective density for different sizes are in good agreement with the hygroscopicity. The dominant peak of effective density distribution appeared at  $\rho_{\text{eff}} = \sim 1.5 \text{ g cm}^{-3}$  for 40 nm particles in the clean period, indicating that they are highly aged with hygroscopic inorganic salts (Yin et al., 2015). As the episode developed, the mean density shifted to lower values, indicating the increasing contribution of [lower density](#)~~less massive~~ carbonaceous materials. The averaged density

distribution was broadened as the episode developed, suggesting that it could be deconvolved into two groups and that the number fraction of the low-density group increased. This finding revealed that the lower density~~less massive~~ particles are less hygroscopic whereas the larger density group corresponds to the more-hygroscopic one. In addition, the variations of hygroscopicity and effective density coincided with the evolution of PBL height, indicating that the increasing accumulation of local emissions due to adverse atmospheric conditions is likely responsible for the enhancement of those near-hydrophobic and lower-density~~less massive~~ particles.

Figure 7 displays the temporal profiles for contributions of EC (including bare EC and OC-coated EC), OC, sulfate, and nitrate determined by SPAMS. Obviously, the relative contribution of nitrate increased as the episode developed. In contrast, the relative contribution of sulfate displayed an opposite trend. This feature is comparable with the aforementioned results of SNA, thus further highlighting the important role of nitrate in haze formation in Shanghai. The number fraction of EC particles generally increased during the haze period, peaking at midnight on January 9 and 10. It should be pointed out that the measured number fraction possibly underestimated the contribution of EC particles because the dominant size range of fresh traffic particles is below the detection limit of SPAMS (0.2–2.0  $\mu\text{m}$ ). This finding provides good support for the increase of near-hydrophobic and less-dense particles as the episode developed. Niu et al. (2016) reported that the number ratio of secondary particles to soot in haze samples was higher than that collected in the clean days in Beijing. Our finding is comparable to their results. In

contrast, the number fraction of pure OC decreased during the pollution event. The possible explanation is that the condensation of organic matter was favored on the large amount of preexisting EC particles, or that photo-oxidation of VOCs was minimized due to lower solar radiation.

### 3.6 Evolutions of hygroscopicity and effective density with particle growth

[As shown in Figure 5](#), ~~Three~~ “banana-shaped” evolutions of the particle size distribution were identified in the representative PM episode. The banana-type contour plot of particle size distributions is a typical characteristics of new particle formation (NPF) events and traditionally regarded as one of the most important criteria for identifying NPF (Xiao et al., 2015; Dal Maso et al., 2005; Levy et al., 2013; Zhang et al., 2012). Atmospheric NPF is often defined by the burst of nucleation mode particles and subsequent growth of the nuclei to larger particles (Zhang et al., 2012; Kulmala et al., 2012). Gas-phase sulfuric acid produced via oxidation of SO<sub>2</sub> by OH radical plays a dominant role in the NPF events. NPF is typically completely suppressed when preexisting particles is abundant, because gas-phase sulfuric acid is rapidly lost to the surfaces of preexisting aerosols (Zhang et al., 2012). In addition to sulfuric acid, low-volatility organic species, and interaction between sulfate and organics are important for NPF (Zhang et al., 2004; Zhao et al., 2009). However, the possibility of NPF can be ignored in this study due to the absence of the burst of nucleation mode particles and the high concentration of PM<sub>1.0</sub>. The burst of Aitken mode particles [in the current study may be](#) ~~was~~ attributable to rapid accumulation of traffic emissions during rush hours under stagnant atmospheric conditions. The “banana-shaped” [particle growth in the](#)

time evolution of particle size distribution from the Aitken mode size range to accumulation mode size range was s-were primarily due tocaused by coagulation and condensation processesgrowth. This feature which provided an excellent opportunity to reveal the chemical mechanism of particle growth during the PM episode.

The first “banana-shaped<sup>d</sup>” evolution of the particle size distribution occurred from approximately 05:00 to 15:00 on January 9, with increase of the particle number concentration ( $N_{\text{total}}$ ) from  $1.7 \times 10^4$  to  $3.4 \times 10^4 \text{ cm}^{-3}$  followed by a decrease trend until 17:00 (Period 1). The second “banana-shaped<sup>d</sup>” evolution occurred from approximately 18:00 on January 9 to approximately 12:00 on January 10 (Period 2). The  $N_{\text{total}}$  increased from  $2.1 \times 10^4$  to  $4.2 \times 10^4 \text{ cm}^{-3}$  within 3 h, followed by gradual decrease of  $N_{\text{total}}$  in contrast to a continuous increase of the particle mass concentration. During the growth process, the mode diameter of the particle population increased from below 40 nm to approximately 200 nm. The third “banana-shaped<sup>d</sup>” evolution began in the evening rush hours on January 10, with the continuous increase of PM mass concentration for 12 h (Period 3). The latter two banana-shaped evolutions lasted long enough to tracer the changes in hygroscopicity and effective density due to particle growth.

Figure 8 illustrates the evolution of particle hygroscopicity and effective density during periods 2 and 3. During the initial stage, the measured GF and effective density distributions were both bimodal, with a dominant peak at  $\text{GF} = \sim 1.0$  and  $\rho_{\text{eff}} = \sim 1.0 \text{ g cm}^{-3}$ , respectively. In a previous study, we found that the number fraction of near-hydrophobic particles varied with the traffic exhaust (Ye et al., 2013). Moreover,

laboratory studies showed that the effective density of 50 nm vehicle particles was approximately 1.0 g cm<sup>-3</sup> (Olfert et al., 2007; Park et al., 2003; Momenimovahed and Olfert, 2015). These findings indicate that the initial burst of Aitken mode particles is attributable to the presence of enhanced traffic-related emissions. In contrast, the number fraction and GF of the more-hygroscopic group increased with [the](#) growing particle size, indicating the addition of hygroscopic inorganic species. The variation of the effective density of the particles was similar to that of the hygroscopicity, indicating the increase of high density materials. In general, inorganic sulfate and nitrate are more hygroscopic and denser than soot particles or organic aerosols (Yin et al., 2015). These findings suggest that secondary sulfate and nitrate increased with the growing particle size, indicating the importance of the conversion of SO<sub>2</sub> and NO<sub>x</sub> in particle growth. This conclusion is supported by the largest SNA concentration in PM<sub>1.0</sub> during the PM episode (31.3 μg m<sup>-3</sup> on January 10 and 23.8 μg m<sup>-3</sup> on January 11). Considering that the concentration of nitrate was much higher than that of sulfate during the haze event, the increase of hygroscopicity was dominated by the addition of nitrate.

#### **4. Conclusions**

Particle size distribution, size-resolved hygroscopic growth and effective density of sub-micrometer aerosols were determined using a HTDMA-APM system, along with measurements of cascade [impactor](#) samples and single particle mass spectrometry in urban Shanghai during winter 2014.

The PM episode exhibited a periodic cycle of ~5 days. The average concentration of PM<sub>2.5</sub> was  $87.2 \pm 67.2 \mu\text{g m}^{-3}$ , with approximately 62% of hourly PM<sub>2.5</sub> concentrations exceeding the Chinese Grade II guideline. Both secondary inorganic salts and carbonaceous aerosols contributed substantially to haze formation, because the mass ratio of  $\text{--SNA/PM}_{1.0}$  fluctuated slightly around 0.28~~ratio was almost constant~~ during the observation period. Nitrate became the most abundant ionic species at PM<sub>1.0</sub> >40  $\mu\text{g m}^{-3}$ , indicating that the sources of nitrate contributed more to haze formation in Shanghai than did SO<sub>2</sub>.

The severe haze pollution was likely triggered by the adverse meteorological conditions, which favored  
the~~caused a large~~ accumulation of local emissions and subsequent rapid growth to larger particles. As the PM episode developed, the number fraction of near-hydrophobic particles of different size increased, consistent with decrease of the mean effective density. Both hygroscopicity and effective density of the particles were found to increase considerably with growing particle size, indicating that secondary aerosol formation was one of the most important contributors~~a major contributor~~ to particle growth. Our results suggest that the accumulation of local emissions under adverse meteorological conditions and subsequent rapid particle growth by secondary processes are primarily responsible for the haze pollution in Shanghai during wintertime.

## Acknowledgments

This work was supported by the National Natural Science Foundation of China (21477020, 21527814,

and 91544224), and the National Science and Technology Support Program of China (2014BAC22B01).

## Reference

- Aggarwal, S. G., Mochida, M., Kitamori, Y., and Kawamura, K.: Chemical closure study on hygroscopic properties of urban aerosol particles in Sapporo, Japan, *Environmental Science & Technology*, 41, 6920-6925, 10.1021/es063092m, 2007.
- Chen, D., Liu, Z., Fast, J., and Ban, J.: Simulations of sulfate-nitrate-ammonium (SNA) aerosols during the extreme haze events over northern China in October 2014, *Atmospheric Chemistry and Physics*, 16, 10707-10724, 10.5194/acp-16-10707-2016, 2016.
- Chu, B., Zhang, X., Liu, Y., He, H., Sun, Y., Jiang, J., Li, J., and Hao, J.: Synergetic formation of secondary inorganic and organic aerosol: effect of SO<sub>2</sub> and NH<sub>3</sub> on particle formation and growth, *Atmospheric Chemistry and Physics*, 16, 14219-14230, 10.5194/acp-16-14219-2016, 2016.
- Dal Maso, M., Kulmala, M., Riipinen, I., Wagner, R., Hussein, T., Aalto, P. P., and Lehtinen, K. E. J.: Formation and growth of fresh atmospheric aerosols: eight years of aerosol size distribution data from SMEAR II, Hyytiälä, Finland, *Boreal Environment Research*, 10, 323-336, 2005.
- Dinar, E., Mentel, T. F., and Rudich, Y.: The density of humic acids and humic like substances (HULIS) from fresh and aged wood burning and pollution aerosol particles, *Atmos. Chem. Phys.*, 6, 5213-5224, 2006.
- Fu, Q. Y., Zhuang, G. S., Wang, J., Xu, C., Huang, K., Li, J., Hou, B., Lu, T., and Streets, D. G.: Mechanism of formation of the heaviest pollution episode ever recorded in the Yangtze River Delta, China, *Atmospheric Environment*, 42, 2023-2036, 2008.
- Gasparini, R., Li, R. J., Collins, D. R., Ferrare, R. A., and Brackett, V. G.: Application of aerosol hygroscopicity measured at the Atmospheric Radiation Measurement Program's Southern Great Plains site to examine composition and evolution, *J. Geophys. Res.-Atmos.*, 111, D05S12, doi:10.1029/2004JD005448, 10.1029/2004jd005448, 2006.
- Guan, W. J., Zheng, X. Y., Chung, K. F., and Zhong, N. S.: Impact of air pollution on the burden of chronic respiratory diseases in China: time for urgent action, *Lancet*, 388, 1939-1951, 2016.
- Guo, S., Hu, M., Guo, Q., Zhang, X., Schauer, J. J., and Zhang, R.: Quantitative evaluation of emission controls on primary and secondary organic aerosol sources during Beijing 2008 Olympics, *Atmospheric Chemistry and Physics*, 13, 8303-8314, 10.5194/acp-13-8303-2013, 2013.
- Guo, S., Hu, M., Zamora, M. L., Peng, J., Shang, D., Zheng, J., Du, Z., Wu, Z., Shao, M., Zeng, L., Molina, M. J., and Zhang, R.: Elucidating severe urban haze formation in China, *Proceedings of the National*

Academy of Sciences of the United States of America, 111, 17373-17378, 10.1073/pnas.1419604111, 2014.

Gysel, M., Crosier, J., Topping, D. O., Whitehead, J. D., Bower, K. N., Cubison, M. J., Williams, P. I., Flynn, M. J., McFiggans, G. B., and Coe, H.: Closure study between chemical composition and hygroscopic growth of aerosol particles during TORCH2, *Atmospheric Chemistry and Physics*, 7, 6131-6144, 2007.

Gysel, M., McFiggans, G. B., and Coe, H.: Inversion of tandem differential mobility analyser (TDMA) measurements, *Journal of Aerosol Science*, 40, 134-151, 10.1016/j.jaerosci.2008.07.013, 2009.

Han, B., Zhang, R., Yang, W., Bai, Z., Ma, Z., and Zhang, W.: Heavy haze episodes in Beijing during January 2013: Inorganic ion chemistry and source analysis using highly time-resolved measurements from an urban site, *Science of The Total Environment*, 544, 319-329, <http://dx.doi.org/10.1016/j.scitotenv.2015.10.053>, 2016.

Heal, M. R., Kumar, P., and Harrison, R. M.: Particles, air quality, policy and health, *Chemical Society Reviews*, 41, 6606-6630, 10.1039/c2cs35076a, 2012.

Hu, M., Peng, J., Sun, K., Yue, D., Guo, S., Wiedensohler, A., and Wu, Z.: Estimation of size-resolved ambient particle density based on the measurement of aerosol number, mass, and chemical size distributions in the winter in Beijing, *Environ Sci Technol*, 46, 9941-9947, 10.1021/es204073t, 2012.

Hu, Q. Q., Fu, H. B., Wang, Z. Z., Kong, L. D., Chen, M. D., and Chen, J. M.: The variation of characteristics of individual particles during the haze evolution in the urban Shanghai atmosphere, *Atmospheric Research*, 181, 95-105, 10.1016/j.atmosres.2016.06.016, 2016.

Huang, R.-J., Zhang, Y., Bozzetti, C., Ho, K.-F., Cao, J.-J., Han, Y., Daellenbach, K. R., Slowik, J. G., Platt, S. M., Canonaco, F., Zotter, P., Wolf, R., Pieber, S. M., Bruns, E. A., Crippa, M., Ciarelli, G., Piazzalunga, A., Schwikowski, M., Abbazade, G., Schnelle-Kreis, J., Zimmermann, R., An, Z., Szidat, S., Baltensperger, U., El Haddad, I., and Prevot, A. S. H.: High secondary aerosol contribution to particulate pollution during haze events in China, *Nature*, 514, 218-222, 10.1038/nature13774, 2014.

IPCC: *Climate Change 2013: The Physical Science Basis*, Cambridge, UK, 2013.

Khalizov, A. F., Xue, H., Wang, L., Zheng, J., and Zhang, R.: Enhanced Light Absorption and Scattering by Carbon Soot Aerosol Internally Mixed with Sulfuric Acid, *Journal of Physical Chemistry A*, 113, 1066-1074, 10.1021/jp807531n, 2009.

Kulmala, M., Petaja, T., Nieminen, T., Sipila, M., Manninen, H. E., Lehtipalo, K., Dal Maso, M., Aalto, P. P., Junninen, H., Paasonen, P., Riipinen, I., Lehtinen, K. E., Laaksonen, A., and Kerminen, V. M.: Measurement of the nucleation of atmospheric aerosol particles, *Nature protocols*, 7, 1651-1667, 10.1038/nprot.2012.091, 2012.

Levy, M. E., Zhang, R. Y., Khalizov, A. F., Zheng, J., Collins, D. R., Glen, C. R., Wang, Y., Yu, X. Y., Luke, W., Jayne, J. T., and Olaguer, E.: Measurements of submicron aerosols in Houston, Texas during

the 2009 SHARP field campaign, *J. Geophys. Res.-Atmos.*, 118, 10518-10534, 10.1002/jgrd.50785, 2013.

Levy, M. E., Zhang, R. Y., Zheng, J., Tan, H. B., Wang, Y., Molina, L. T., Takahama, S., Russell, L. M., and Li, G. H.: Measurements of submicron aerosols at the California-Mexico border during the Cal-Mex 2010 field campaign, *Atmospheric Environment*, 88, 308-319, 10.1016/j.atmosenv.2013.08.062, 2014.

Li, J. J., Wang, G. H., Ren, Y. Q., Wang, J. Y., Wu, C., Han, Y. N., Zhang, L., Cheng, C. L., and Meng, J. J.: Identification of chemical compositions and sources of atmospheric aerosols in Xi'an, inland China during two types of haze events, *Science of the Total Environment*, 566, 230-237, 10.1016/j.scitotenv.2016.05.057, 2016.

Li, L., Huang, Z. X., Dong, J. G., Li, M., Gao, W., Nian, H. Q., Fu, Z., Zhang, G. H., Bi, X. H., Cheng, P., and Zhou, Z.: Real time bipolar time-of-flight mass spectrometer for analyzing single aerosol particles, *International Journal of Mass Spectrometry*, 303, 118-124, 10.1016/j.ijms.2011.01.017, 2011.

Li, P., Yan, R., Yu, S., Wang, S., Liu, W., and Bao, H.: Reinstate regional transport of PM<sub>2.5</sub> as a major cause of severe haze in Beijing, *Proceedings of the National Academy of Sciences of the United States of America*, 112, E2739-E2740, 10.1073/pnas.1502596112, 2015.

Lin, Y., Huang, K., Zhuang, G., Fu, J. S., Wang, Q., Liu, T., Deng, C., and Fu, Q.: A multi-year evolution of aerosol chemistry impacting visibility and haze formation over an Eastern Asia megacity, Shanghai, *Atmospheric Environment*, 92, 76-86, 10.1016/j.atmosenv.2014.04.007, 2014.

Liu, H. J., Zhao, C. S., Nekat, B., Ma, N., Wiedensohler, A., van Pinxteren, D., Spindler, G., Muller, K., and Herrmann, H.: Aerosol hygroscopicity derived from size-segregated chemical composition and its parameterization in the North China Plain, *Atmos. Chem. Phys.*, 14, 2525-2539, 10.5194/acp-14-2525-2014, 2014.

Malloy, Q. G. J., Nakao, S., Qi, L., Austin, R., Stothers, C., Hagino, H., and Cocker, D. R.: Real-Time Aerosol Density Determination Utilizing a Modified Scanning Mobility Particle Sizer Aerosol Particle Mass Analyzer System, *Aerosol Sci. Technol.*, 43, 673-678, Pii 910340704 10.1080/02786820902832960, 2009.

Massling, A., Stock, M., Wehner, B., Wu, Z. J., Hu, M., Brüggemann, E., Gnauk, T., Herrmann, H., and Wiedensohler, A.: Size segregated water uptake of the urban submicrometer aerosol in Beijing, *Atmospheric Environment*, 43, 1578-1589, 2009.

Momenimovahed, A., and Olfert, J. S.: Effective density and volatility of particles emitted from gasoline direct injection vehicles and implications for particle mass measurement, *Aerosol Sci. Technol.*, 49, 1051-1062, 10.1080/02786826.2015.1094181, 2015.

Niu, H. Y., Hu, W., Zhang, D. Z., Wu, Z. J., Guo, S., Pian, W., Cheng, W. J., and Hu, M.: Variations of fine particle physiochemical properties during a heavy haze episode in the winter of Beijing, *Science of the Total Environment*, 571, 103-109, 10.1016/j.scitotenv.2016.07.147, 2016.

Olfert, J. S., Symonds, J. P. R., and Collings, N.: The effective density and fractal dimension of particles

emitted from a light-duty diesel vehicle with a diesel oxidation catalyst, *Journal of Aerosol Science*, 38, 69-82, 10.1016/j.jaerosci.2006.10.002, 2007.

Pagels, J., Khalizov, A. F., McMurry, P. H., and Zhang, R. Y.: Processing of Soot by Controlled Sulphuric Acid and Water Condensation Mass and Mobility Relationship, *Aerosol Sci. Technol.*, 43, 629-640, 10.1080/02786820902810685, 2009.

Park, K., F. C., Kittelson, D. B., and McMurry, P. H.: Relationship between particle mass and mobility for diesel exhaust particles *Environmental Science and Technology*, 37, 577-583, 2003.

Peng, J., Hu, M., Guo, S., Du, Z., Zheng, J., Shang, D., Zamora, M. L., Zeng, L., Shao, M., Wu, Y.-S., Zheng, J., Wang, Y., Glen, C. R., Collins, D. R., Molina, M. J., and Zhang, R.: Markedly enhanced absorption and direct radiative forcing of black carbon under polluted urban environments, *Proceedings of the National Academy of Sciences of the United States of America*, 113, 4266-4271, 10.1073/pnas.1602310113, 2016.

Petters, M. D., and Kreidenweis, S. M.: A single parameter representation of hygroscopic growth and cloud condensation nucleus activity, *Atmospheric Chemistry and Physics*, 7, 1961-1971, 2007.

Qiao, T., Zhao, M., Xiu, G., and Yu, J.: Simultaneous monitoring and compositions analysis of PM<sub>1</sub> and PM<sub>2.5</sub> in Shanghai: Implications for characterization of haze pollution and source apportionment, *The Science of the total environment*, 557-558, 386-394, 10.1016/j.scitotenv.2016.03.095, 2016.

Rissler, J., Nordin, E. Z., Eriksson, A. C., Nilsson, P. T., Frosch, M., Sporre, M. K., Wierzbicka, A., Svenningsson, B., Londahl, J., Messing, M. E., Sjogren, S., Hemmingsen, J. G., Loft, S., Pagels, J. H., and Swietlicki, E.: Effective Density and Mixing State of Aerosol Particles in a Near-Traffic Urban Environment, *Environmental science & technology*, 48, 6300-6308, 10.1021/es5000353, 2014.

Shi, Y., Chen, J., Hu, D., Wang, L., Yang, X., and Wang, X.: Airborne submicron particulate (PM<sub>1</sub>) pollution in Shanghai, China: Chemical variability, formation/dissociation of associated semi-volatile components and the impacts on visibility, *Science of the Total Environment*, 473, 199-206, 10.1016/j.scitotenv.2013.12.024, 2014.

Spencer, M. T., Shields, L. G., and Prather, K. A.: Simultaneous measurement of the effective density and chemical composition of ambient aerosol particles, *Environmental Science & Technology*, 41, 1303-1309, 10.1021/es061425+, 2007.

Sun, Y. L., Chen, C., Zhang, Y. J., Xu, W. Q., Zhou, L. B., Cheng, X. L., Zheng, H. T., Ji, D. S., Li, J., Tang, X., Fu, P. Q., and Wang, Z. F.: Rapid formation and evolution of an extreme haze episode in Northern China during winter 2015, *Scientific Reports*, 6, 10.1038/srep27151, 2016.

Swietlicki, E., Hansson, H. C., Hameri, K., Svenningsson, B., Massling, A., McFiggans, G., McMurry, P. H., Petaja, T., Tunved, P., Gysel, M., Topping, D., Weingartner, E., Baltensperger, U., Rissler, J., Wiedensohler, A., and Kulmala, M.: Hygroscopic properties of submicrometer atmospheric aerosol particles measured with H-TDMA instruments in various environments - a review, *Tellus Ser. B-Chem.*

Phys. Meteorol., 60, 432-469, 10.1111/j.1600-0889.2008.00350.x, 2008.

Tao, Y., Ye, X. N., Ma, Z., Xie, Y. Y., Wang, R. Y., Chen, J. M., Yang, X., and Jiang, S. Q.: Insights into different nitrate formation mechanisms from seasonal variations of secondary inorganic aerosols in Shanghai, *Atmospheric Environment*, 145, 1-9, 10.1016/j.atmosenv.2016.09.012, 2016.

Topping, D. O., McFiggans, G. B., and Coe, H.: A curved multi-component aerosol hygroscopicity model framework: Part 1 - Inorganic compounds, *Atmospheric Chemistry and Physics*, 5, 1205-1222, 2005.

Turpin, B. J., and Lim, H. J.: Species contributions to PM<sub>2.5</sub> mass concentrations: Revisiting common assumptions for estimating organic mass, *Aerosol Sci. Technol.*, 35, 602-610, 10.1080/02786820152051454, 2001.

Wang, G., Zhang, R., Gomez, M. E., Yang, L., Zamora, M. L., Hu, M., Lin, Y., Peng, J., Guo, S., Meng, J., Li, J., Cheng, C., Hu, T., Ren, Y., Wang, Y., Gao, J., Cao, J., An, Z., Zhou, W., Li, G., Wang, J., Tian, P., Marrero-Ortiz, W., Secrest, J., Du, Z., Zheng, J., Shang, D., Zeng, L., Shao, M., Wang, W., Huang, Y., Wang, Y., Zhu, Y., Li, Y., Hu, J., Pan, B., Cai, L., Cheng, Y., Ji, Y., Zhang, F., Rosenfeld, D., Liss, P. S., Duce, R. A., Kolb, C. E., and Molina, M. J.: Persistent sulfate formation from London Fog to Chinese haze, *Proceedings of the National Academy of Sciences of the United States of America*, 113, 13630-13635, 10.1073/pnas.1616540113, 2016.

Wang, H., Xu, J., Zhang, M., Yang, Y., Shen, X., Wang, Y., Chen, D., and Guo, J.: A study of the meteorological causes of a prolonged and severe haze episode in January 2013 over central-eastern China, *Atmospheric Environment*, 98, 146-157, 10.1016/j.atmosenv.2014.08.053, 2014a.

Wang, Y., Wan, Q., Meng, W., Liao, F., Tan, H., and Zhang, R.: Long-term impacts of aerosols on precipitation and lightning over the Pearl River Delta megacity area in China, *Atmospheric Chemistry and Physics*, 11, 12421-12436, 10.5194/acp-11-12421-2011, 2011.

Wang, Y., Khalizov, A., Levy, M., and Zhang, R.: New Directions: Light absorbing aerosols and their atmospheric impacts, *Atmospheric Environment*, 81, 713-715, 10.1016/j.atmosenv.2013.09.034, 2013.

Wang, Y., Zhang, Q., Jiang, J., Zhou, W., Wang, B., He, K., Duan, F., Zhang, Q., Philip, S., and Xie, Y.: Enhanced sulfate formation during China's severe winter haze episode in January 2013 missing from current models, *J. Geophys. Res.-Atmos.*, 119, 10.1002/2013jd021426, 2014b.

Wang, Y., Zhang, R., and Saravanan, R.: Asian pollution climatically modulates mid-latitude cyclones following hierarchical modelling and observational analysis, *Nature Communications*, 5, 10.1038/ncomms4098, 2014c.

Wang, Y. H., Liu, Z. R., Zhang, J. K., Hu, B., Ji, D. S., Yu, Y. C., and Wang, Y. S.: Aerosol physicochemical properties and implications for visibility during an intense haze episode during winter in Beijing, *Atmospheric Chemistry and Physics*, 15, 3205-3215, 10.5194/acp-15-3205-2015, 2015.

Wu, G., Li, Z., Fu, C., Zhang, X., Zhang, R., Zhang, R., Zhou, T., Li, J., Li, J., Zhou, D., Wu, L., Zhou, L., He, B., and Huang, R.: Advances in studying interactions between aerosols and monsoon in China,

Science China-Earth Sciences, 59, 1-16, 10.1007/s11430-015-5198-z, 2016a.

Wu, S., Ni, Y., Li, H., Pan, L., Yang, D., Baccarelli, A. A., Deng, F., Chen, Y., Shima, M., and Guo, X.: Short-term exposure to high ambient air pollution increases airway inflammation and respiratory symptoms in chronic obstructive pulmonary disease patients in Beijing, China, *Environment International*, 94, 76-82, 10.1016/j.envint.2016.05.004, 2016b.

Wu, Z. J., Zheng, J., Shang, D. J., Du, Z. F., Wu, Y. S., Zeng, L. M., Wiedensohler, A., and Hu, M.: Particle hygroscopicity and its link to chemical composition in the urban atmosphere of Beijing, China, during summertime, *Atmos. Chem. Phys.*, 16, 1123-1138, 10.5194/acp-16-1123-2016, 2016c.

Xiao, S., Wang, Q. Y., Cao, J. J., Huang, R. J., Chen, W. D., Han, Y. M., Xu, H. M., Liu, S. X., Zhou, Y. Q., Wang, P., Zhang, J. Q., and Zhan, C. L.: Long-term trends in visibility and impacts of aerosol composition on visibility impairment in Baoji, China, *Atmospheric Research*, 149, 88-95, 10.1016/j.atmosres.2014.06.006, 2014.

Xiao, S., Wang, M. Y., Yao, L., Kulmala, M., Zhou, B., Yang, X., Chen, J. M., Wang, D. F., Fu, Q. Y., Worsnop, D. R., and Wang, L.: Strong atmospheric new particle formation in winter in urban Shanghai, China, *Atmospheric Chemistry and Physics*, 15, 1769-1781, 10.5194/acp-15-1769-2015, 2015.

Xie, Y., Ding, A., Nie, W., Mao, H., Qi, X., Huang, X., Xu, Z., Kerminen, V.-M., Petaja, T., Chi, X., Virkkula, A., Boy, M., Xue, L., Guo, J., Sun, J., Yang, X., Kulmala, M., and Fu, C.: Enhanced sulfate formation by nitrogen dioxide: Implications from in situ observations at the SORPES station, *J. Geophys. Res.-Atmos.*, 120, 12679-12694, 10.1002/2015jd023607, 2015.

Yang, L., Zhou, X., Wang, Z., Zhou, Y., Cheng, S., Xu, P., Gao, X., Nie, W., Wang, X., and Wang, W.: Airborne fine particulate pollution in Jinan, China: Concentrations, chemical compositions and influence on visibility impairment, *Atmospheric Environment*, 55, 506-514, 10.1016/j.atmosenv.2012.02.029, 2012.

Ye, X. N., Chen, T. Y., Hu, D. W., Yang, X., Chen, J. M., Zhang, R. Y., Khakuziv, A. F., and Wang, L.: A multifunctional HTDMA system with a robust temperature control, *Advances in Atmospheric Sciences*, 26, 1235-1240, 10.1007/s00376-009-8134-3, 2009.

Ye, X. N., Ma, Z., Hu, D. W., Yang, X., and Chen, J. M.: Size-resolved hygroscopicity of submicrometer urban aerosols in Shanghai during wintertime, *Atmospheric Research*, 99, 353-364, 2010.

Ye, X. N., Ma, Z., Zhang, J. C., Du, H. H., Chen, J. M., Chen, H., Yang, X., Gao, W., and Geng, F. H.: Important role of ammonia on haze formation in Shanghai, *Environ Res Lett*, 6, Artn 024019 Doi 10.1088/1748-9326/6/2/024019, 2011.

Ye, X. N., Tang, C., Yin, Z., Chen, J. M., Ma, Z., Kong, L. D., Yang, X., Gao, W., and Geng, F. H.: Hygroscopic growth of urban aerosol particles during the 2009 Mirage-Shanghai Campaign, *Atmospheric Environment*, 64, 263-269, 10.1016/j.atmosenv.2012.09.064, 2013.

Yin, Z., Ye, X., Jiang, S., Tao, Y., Shi, Y., Yang, X., and Chen, J.: Size-resolved effective density of urban aerosols in Shanghai, *Atmospheric Environment*, 100, 133-140, 10.1016/j.atmosenv.2014.10.055, 2015.

Zhang, Q., Quan, J., Tie, X., Li, X., Liu, Q., Gao, Y., and Zhao, D.: Effects of meteorology and secondary particle formation on visibility during heavy haze events in Beijing, China, *Science of The Total Environment*, 502, 578-584, <http://dx.doi.org/10.1016/j.scitotenv.2014.09.079>, 2015a.

Zhang, R., Khalizov, A., Wang, L., Hu, M., and Xu, W.: Nucleation and Growth of Nanoparticles in the Atmosphere, *Chemical Reviews*, 112, 1957-2011, 10.1021/cr2001756, 2012.

Zhang, R., Guo, S., Zamora, M. L., and Hu, M.: Reply to Li et al.: Insufficient evidence for the contribution of regional transport to severe haze formation in Beijing, *Proceedings of the National Academy of Sciences of the United States of America*, 112, E2741-E2741, 10.1073/pnas.1503855112, 2015b.

Zhang, R., Wang, G., Guo, S., Zamora, M. L., Ying, Q., Lin, Y., Wang, W., Hu, M., and Wang, Y.: Formation of Urban Fine Particulate Matter, *Chemical Reviews*, 115, 3803-3855, 10.1021/acs.chemrev.5b00067, 2015c.

Zhang, R. Y., Suh, I., Zhao, J., Zhang, D., Fortner, E. C., Tie, X. X., Molina, L. T., and Molina, M. J.: Atmospheric new particle formation enhanced by organic acids, *Science*, 304, 1487-1490, 10.1126/science.1095139, 2004.

Zhang, R. Y., Khalizov, A. F., Pagels, J., Zhang, D., Xue, H. X., and McMurry, P. H.: Variability in morphology, hygroscopicity, and optical properties of soot aerosols during atmospheric processing, *Proceedings of the National Academy of Sciences of the United States of America*, 105, 10291-10296, 2008.

Zhao, J., Khalizov, A., Zhang, R., and McGraw, R.: Hydrogen-Bonding Interaction in Molecular Complexes and Clusters of Aerosol Nucleation Precursors, *Journal of Physical Chemistry A*, 113, 680-689, 10.1021/jp806693r, 2009.

Zhao, X. J., Zhao, P. S., Xu, J., Meng, W., Pu, W. W., Dong, F., He, D., and Shi, Q. F.: Analysis of a winter regional haze event and its formation mechanism in the North China Plain, *Atmospheric Chemistry and Physics*, 13, 5685-5696, 10.5194/acp-13-5685-2013, 2013.

Zheng, G. J., Duan, F. K., Su, H., Ma, Y. L., Cheng, Y., Zheng, B., Zhang, Q., Huang, T., Kimoto, T., Chang, D., Poeschl, U., Cheng, Y. F., and He, K. B.: Exploring the severe winter haze in Beijing: the impact of synoptic weather, regional transport and heterogeneous reactions, *Atmospheric Chemistry and Physics*, 15, 2969-2983, 10.5194/acp-15-2969-2015, 2015.

## Figure and Table Captions

Figure 1 Schematic diagram of HTDMA-APM system.

Figure 2. Temporal evolutions of  $PM_{1.0}$ ,  $PM_{2.5}$ , and  $PM_{10}$  concentrations during the winter observation.

Figure 3 Variations of sulfate, nitrate, and ammonium concentrations as a function of  $PM_{1.0}$  mass loading.

Figure 4 Box plots showing hygroscopicity parameter and effective density at each dry diameter over the whole observation. The whiskers represent the 5<sup>th</sup> and 95<sup>th</sup> percentile, the two borders of box display the 25<sup>th</sup> and 75<sup>th</sup> percentile, and the band in each box denotes the median.

Figure 5 Temporal evolutions of particle number size distribution (A), volume size distribution (B), total number concentration and total volume concentration (C), and  $PM_{1.0}$  concentration and calculated PM (less than 600 nm in mobility diameter) concentration during the representative PM episode from 7 to 12 January.

Figure 6 Evolutions of particle hygroscopic growth factor and effective density for different sizes during the representative PM episode.

Figure 7 Temporal evolutions of chemical compositions determined by SPAMS during the representative PM episode.

Figure 8 Particle hygroscopicity and density during the two particle growth processes

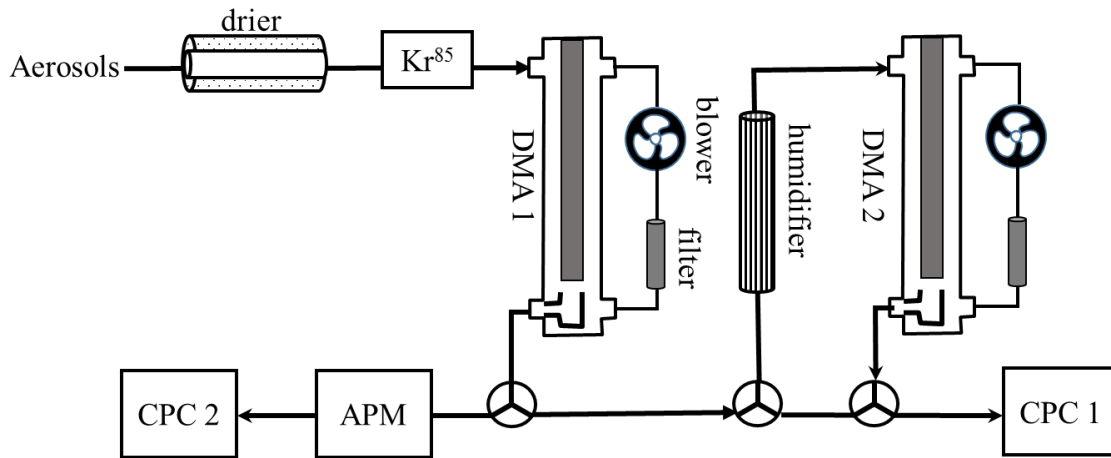


Figure 1 Schematic diagram of HTDMA-APM system.

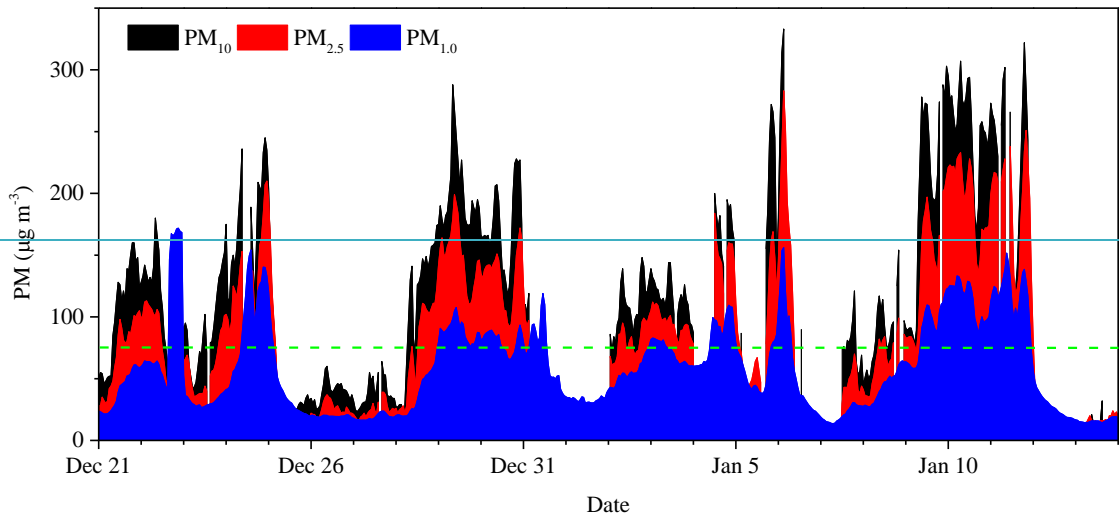
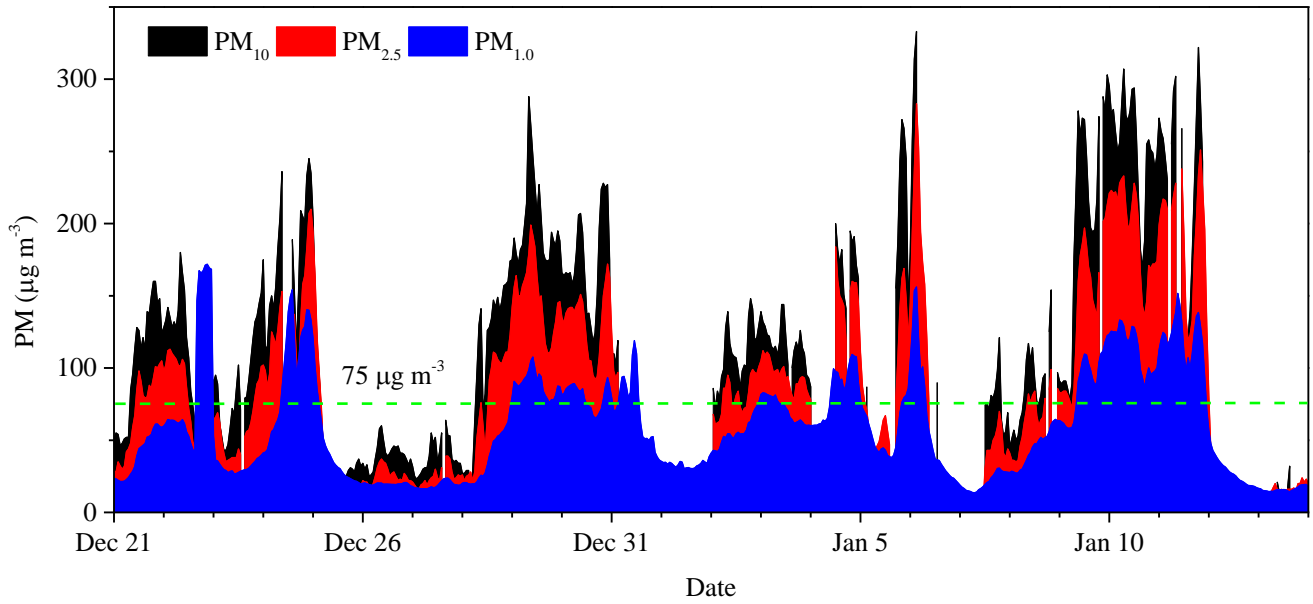
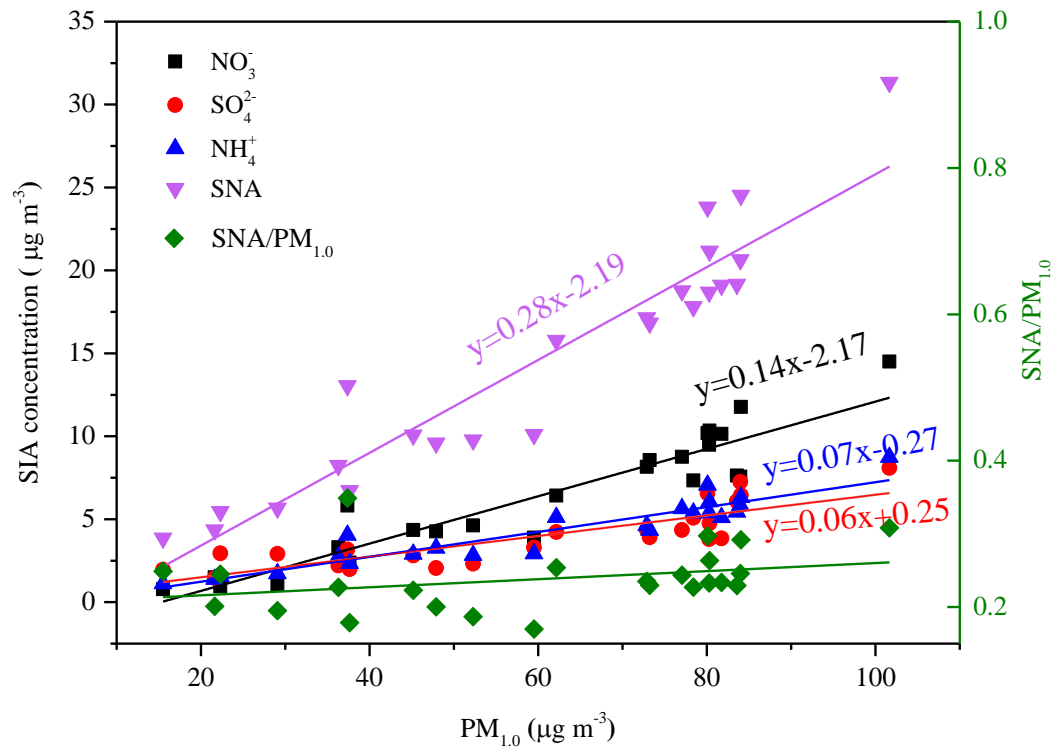


Figure 2. Temporal evolutions of  $\text{PM}_{1.0}$ ,  $\text{PM}_{2.5}$ , and  $\text{PM}_{10}$  concentrations during the winter observation.



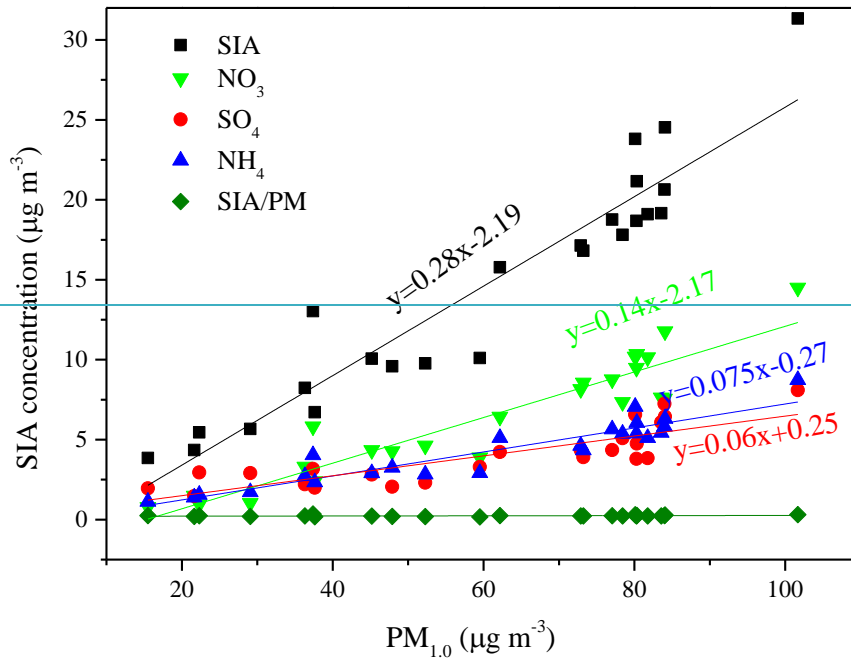


Figure 3 Variations of sulfate, nitrate, and ammonium concentrations as a function of PM<sub>1.0</sub> mass loading.

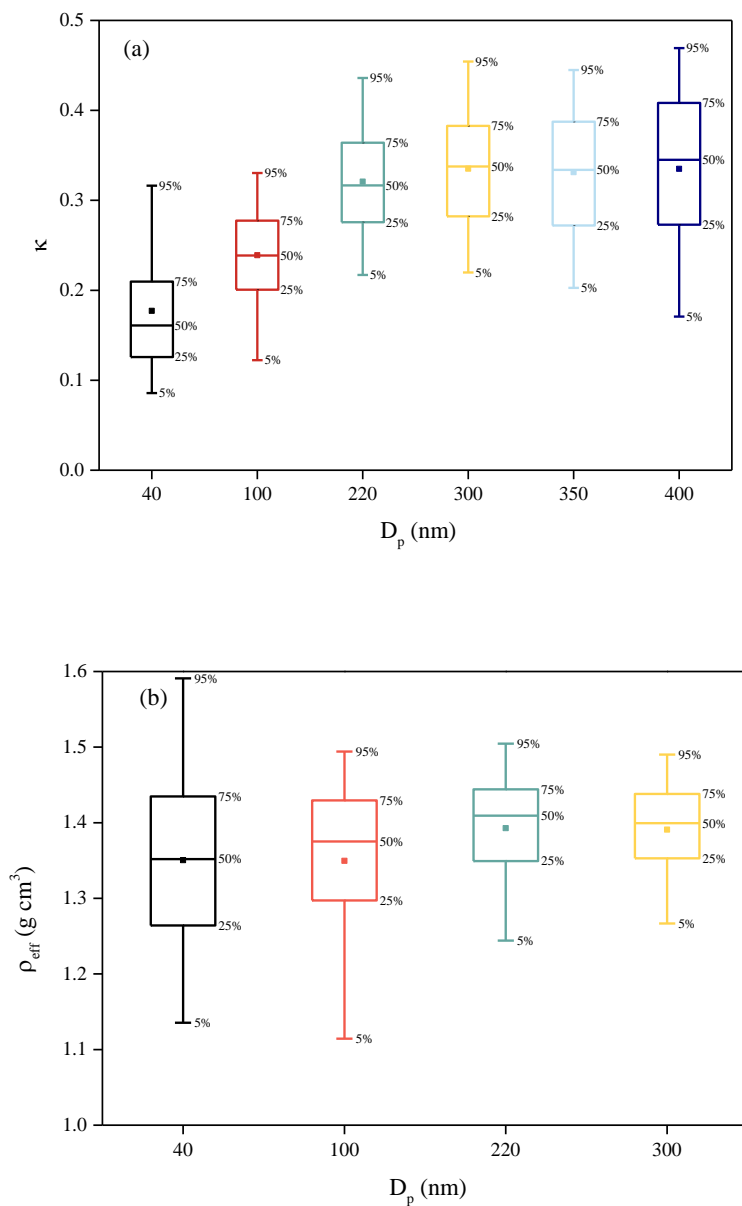


Figure 4 Box plots showing hygroscopicity parameter and effective density at each dry diameter over the whole observation. The whiskers represent the 5<sup>th</sup> and 95<sup>th</sup> percentile, the two borders of box display the 25<sup>th</sup> and 75<sup>th</sup> percentile, and the band in each box denotes the median.

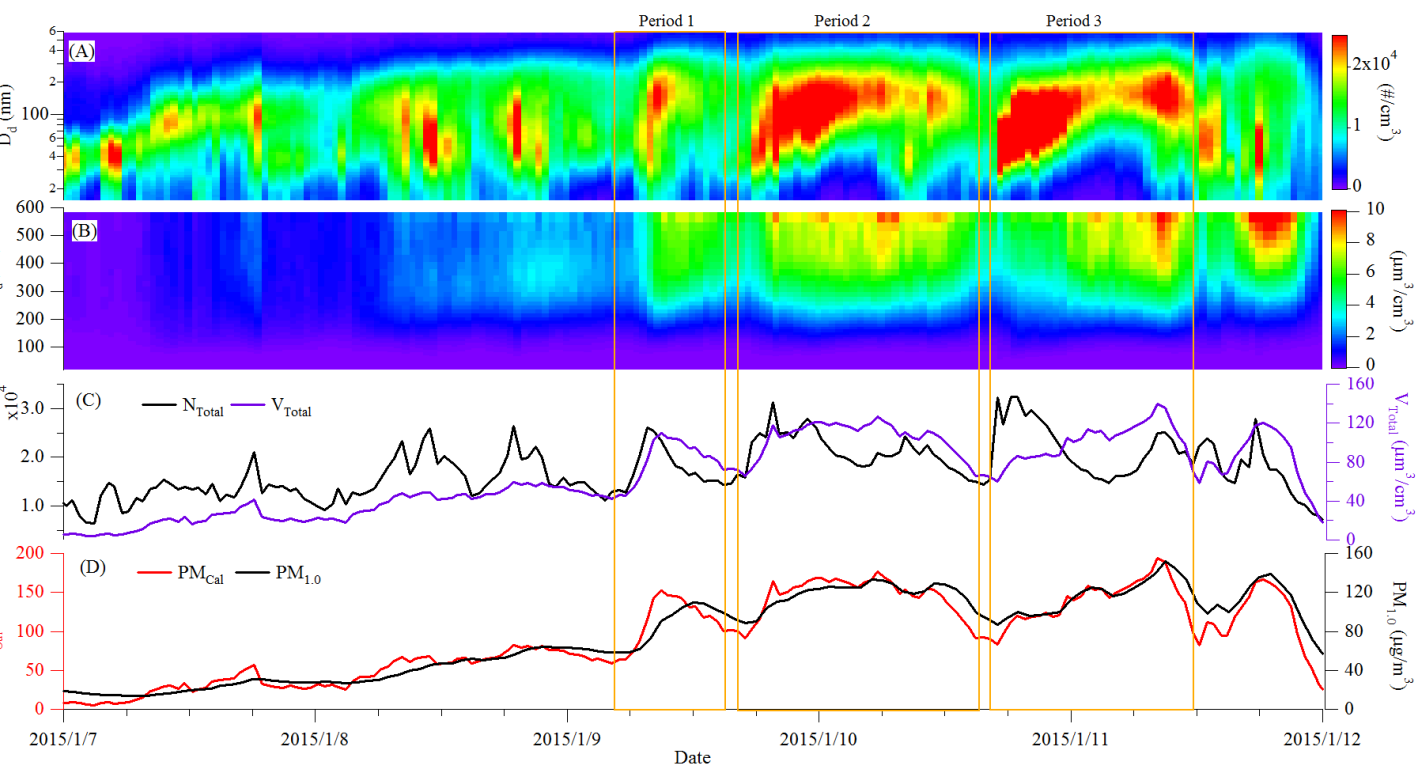


Figure 5 Temporal evolutions of particle number size distribution (A), volume size distribution (B), total number concentration and total volume concentration (C), and  $\text{PM}_{1.0}$  concentration and calculated PM (less than 600 nm in mobility diameter) concentration during the representative PM episode from 7 to 12 January.

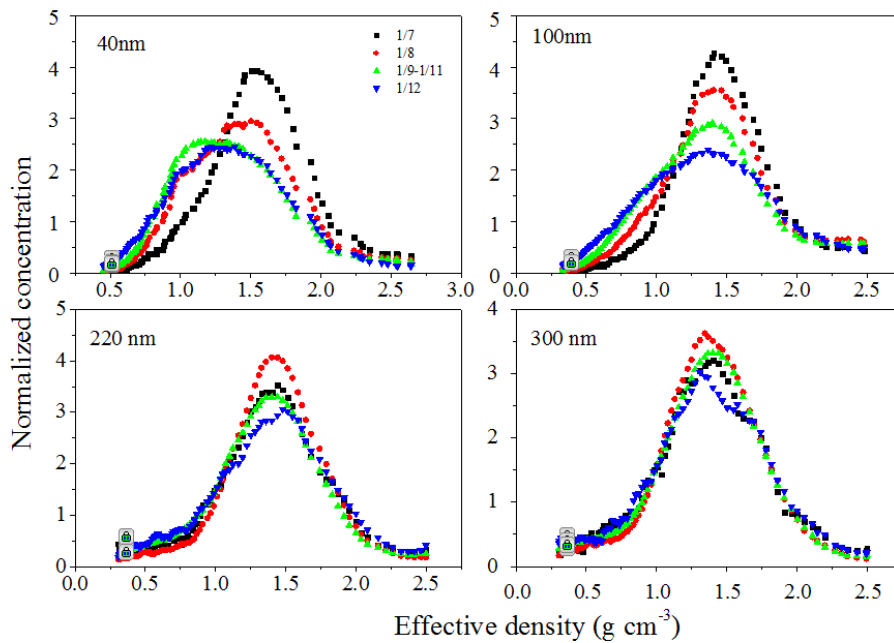
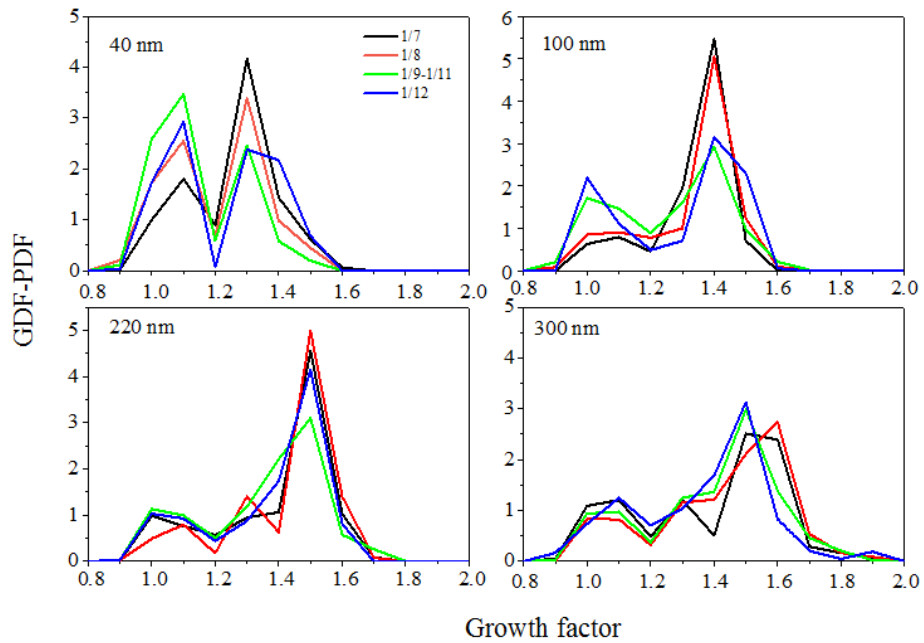


Figure 6 Evolutions of particle hygroscopic growth factor and effective density for different sizes during the representative PM episode.

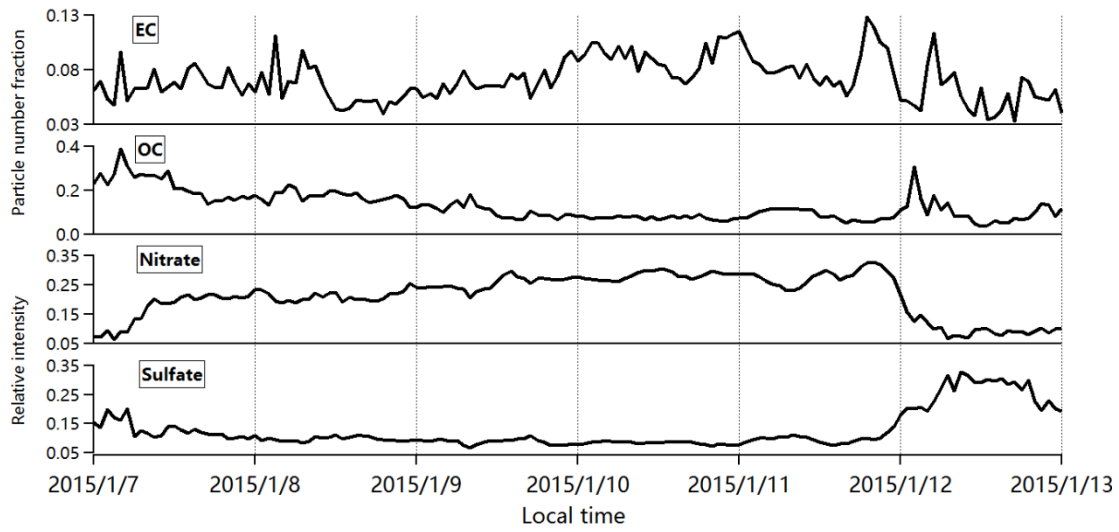


Figure 7 Temporal evolutions of chemical compositions determined by SPAMS during the representative PM episode.

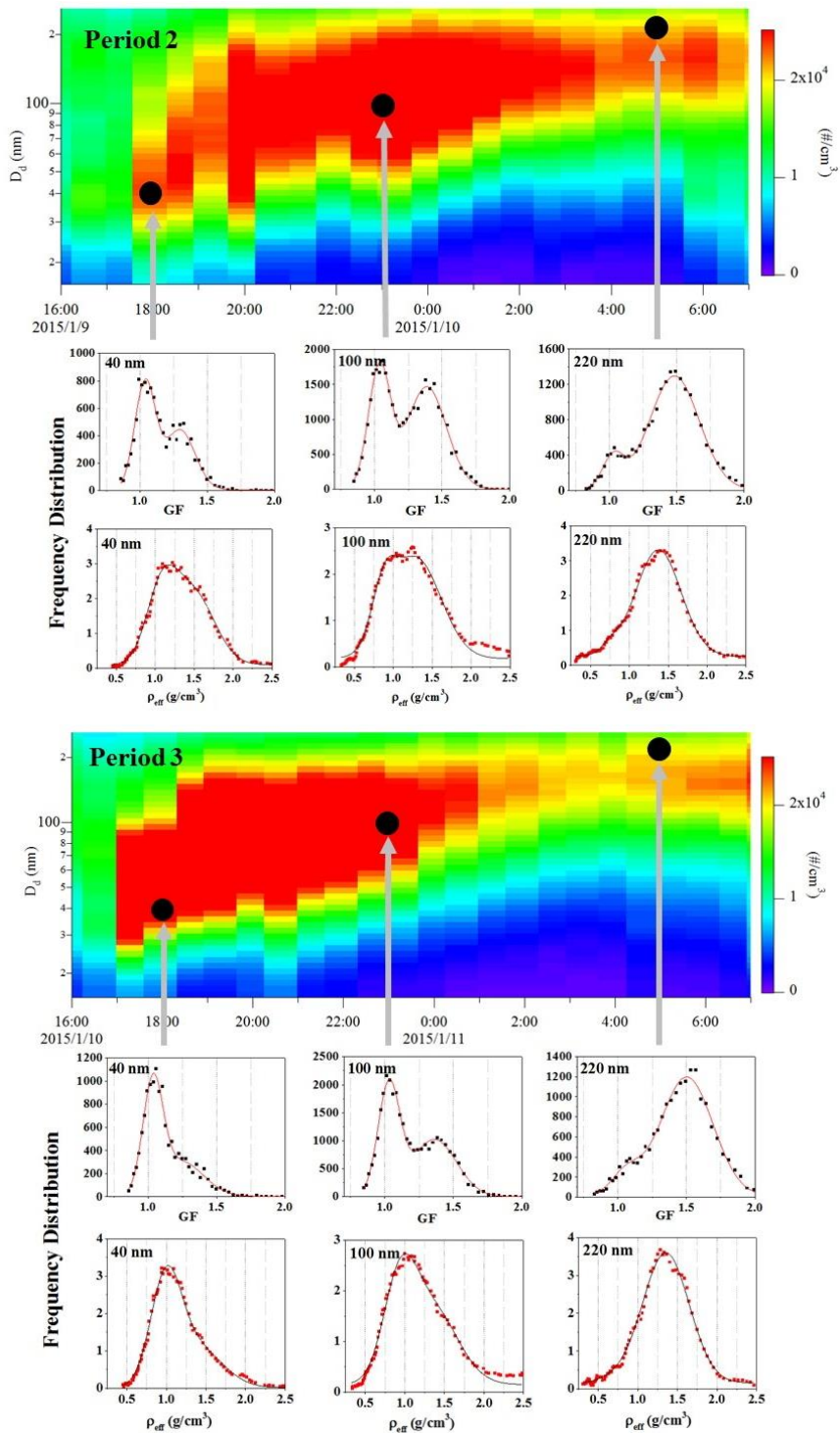


Figure 8 Particle hygroscopicity and density during the two particle growth processes.